Cleaner and Responsible Consumption 5 (2022) 100069

Contents lists available at ScienceDirect

Cleaner and Responsible Consumption

journal homepage: www.journals.elsevier.com/cleaner-and-responsible-consumption

Using artificial intelligence models and degree-days method to estimate the heat consumption evolution of a building stock until 2050: A case study in a temperate climate of the Northern part of Europe

Antoinette Marie Reine Nishimwe *, Sigrid Reiter

LEMA Research Group, Urban & Environmental Engineering Department, University of Liège, Allée de La Découverte 9, Quartier Polytech 1, 4000, Liège, Belgium

ARTICLE INFO

Keywords:
AI modelling
ML and DL models
Heating degree-days estimation
Heat consumption forecasting
City scale

ABSTRACT

The energy use in buildings is highly influenced by outdoor temperature changes. In the contest of nowadays climate change, its impact on the energy sector is important and needs to be assessed. This study investigates how the heat consumption (HC) of the existing regional building stock, located in a temperate climate in the Northern part of Europe (Belgium), will be influenced by future climate changes. First, the Seasonal Auto-Regressive Integrated Moving Average (SARIMA), Long Short-Term Memory (LSTM) and Gated Recurrent Unit (GRU) models are used to predict the temperature until 2050 from historical data. Second, the UK Met Office equations are applied for computing the heating degree-days (HDD) considering the base temperature of 15°C. Finally, the HC of this building stock is projected until 2050 using the degree-days (DD) method. The decrease in HDD is about −11.76% from 2012 to 2050. The HC reduction, calculated at the regional scale, is reaching −8.82 %, −10.00%, and −11.26% for respectively residential, tertiary, and industrial buildings. The calculated HC is mapped on municipality, urban region, and province scales. The produced maps will help decision-makers set up efficient energy management strategies. The used methods can be replicated in other regions with the same kind of data.

1. Introduction

The actual building stock in Europe represents 40 % of its total energy consumption and is also responsible for 36% of its CO2 emissions (European Commission, 2017). The majority of European buildings are more than 50 years old amongst which nearly 75 % have very low energy efficiency (European Commission, 2018). Therefore, sustainable energy systems and management must be developed for decreasing the heat consumption (HC) of buildings over time. Buildings' HC is influenced by outdoor temperatures and thus will be impacted by climate change. Forecasting the level of HC increase or decrease related to climate change at a regional scale is becoming relevant to properly managing energy uses in existing buildings stocks (Cholewa et al., 2021a). Thus, it is necessary to answer questions about how much heat will be consumed in the future and which factors must be considered to take into account the likely effects of climate change on buildings' HC.

This research studied the influence of climate change on the buildings' HC up to 2050 for nearly 1.7 million buildings, in Wallonia (Belgium), under a temperate climate in the Northern part of Europe. To achieve this goal, historical maximum and minimum temperature data from 1901 to 2019 are used considering the base temperature of 15 °C mostly used in Belgium (RMI, 2021). Innovative statistical models including machine learning (ML) and deep learning (DL) models are widely used to forecast time-series data such as temperature. Due to the rapid development of these new technologies, ML and DL models are known to produce realistic predictions. This article will compare different methods of local temperature forecasting and use the best model for our case study, to assess future temperature change effects on the HC of the studied building stock.

The innovation of this study is the evaluation and analysis of the impact of climate change on HC of a regional building stock including a huge database of nearly 1.7 million buildings. Contrary to many studies that consider one or few buildings, the authors developed a reproducible methodology for HC forecast starting from cadastral data and raw temperature data of a big area which make it possible to assess climate change on energy use at a regional scale. Moreover, all the building types present in the studied Region, namely residential, tertiary and industrial buildings, are considered. The methodological innovation of this research consists of combining an artificial intelligence (AI) model with other recognized scientific methods to produce decision support tools for territorial energy management. The HC visualization of the

* Corresponding author.
E-mail address: marie-reine.nishimwe@uliege.be (A.M.R. Nishimwe).

https://doi.org/10.1016/j.clrc.2022.100069
Received 20 January 2022; Received in revised form 22 April 2022; Accepted 22 May 2022
Available online 30 May 2022

Nomenclature

AI	Artificial Intelligence
AMZ	Alternating Migrant Zones
ANN	Artificial Neural Network
ANFIS	Adaptive neuro-fuzzy inference system
AR	Auto-Regressive
ARIMA	Auto-Regressive Integrated Moving Average
DD	Degree Days
DL	Deep Learning
ERDF	European Regional Development Fund
ETS	Error Trend Seasonality
GHG	Greenhouse Gas
GRU	Gated Recurrent Unit
GWh	Gigawatt hour
HC	Heat Consumption
HDD	Heating Degree Days
LSTM	Long Short Term Memory
MA	Moving Average
MAE	Mean Absolute Error
MAPE	Mean Absolute Percentage Error
MASE	Mean Absolute Scaled Error
ML	Machine Learning
NCDC	National Climate Data Centre
NN	Neural Network
NOAA	National Oceanic and Atmospheric Administration
OAT	Outdoor Air Temperature
RClimdex	tool for daily climate data quality control procedure
RCP	Representative Concentration Pathway
RD	Relative Difference
RMI	Royal Meteorological Institute
RMSE	Root Mean Square Error
RNN	Recurrent Neural Network
SARIMA	Seasonal Auto-Regressive Integrated Moving Average
T_{avg}	Average temperature
T_{base}	Base temperature
T_{max}	Maximum temperature
T_{min}	Minimum temperature
TSA	Time Series Analysis
TWh	Terawatt hour

whole regional building stock on different mapping scales is performed, and its usefulness for efficient energy management and planning is shown. The results are used to identify the relative distribution of the predicted HC for various geographic areas and built morphologies. Moreover, the results allow selecting specific parts of the building stock with higher HC to be targeted in smart energy management programs of different municipalities. Thus, this study will help policymakers and stakeholders to become aware of which type of building morphologies and geographic areas are worth investments to reach national and European Union goals on building energy management. For international researchers, the results are representative of the buildings' HC evolution that could take place in other countries located in a cold temperate climate. Finally, the developed method dedicated to the evaluation, forecast, and spatial analysis of the impact of climate change on buildings' HC of large building stock can be applied in all regions for which data similar to those used in our case study are available, even if the climate and building typology is different.

This article is structured as follows: the study is introduced in section 1, the literature review on cities' energy consumption forecasting is summarized in section 2, the research methodology employed is discussed in section 3, section 4 presents the research results and discussion, then the limitations of the study are detailed in section 5, finally the conclusions of the study and future works are presented in Section 6.

2. Literature review

Climate change remains the main concern of all nations, and the adverse effects of this problem are enormous (Cholewa et al., 2021a; Nematchoua et al., 2018). The heat consumption (HC) is climate-driven. For many years, various weather data such as temperature, pressure, and wind have been integrated into statistical models to describe, analyse and forecast the HC (An đ elkovi ć and Bajatovi ć, 2020; ARAS and ARAS, 2004; Cholewa et al., 2021b). Zhang and Feng recommend that climate data should be quality controlled before further computation and use (Zhang and Yang, 2004). The reason is that climate data are biased by errors from observers and observation equipment failure. The RClimdex is a powerful tool for daily climate data quality control procedures (Zhang and Yang, 2004; ETCCDI, 2020). It detects all unreasonable values in the dataset such as daily maximum temperature less than daily minimum temperature (Zhang and Yang, 2004). The data quality control and cleaning steps are very crucial since the output results from the models depend upon the quality of the input data.

Based on the outdoor air temperature (OAT), Saloux and Candanedo employed the linear regression models to estimate the heating load of 52 residential houses in the Drake Landing Solar Community (Canada) (Saloux and Candanedo, 2018). Their study concluded that the accuracy gained using the machine learning algorithms is relatively small compared to a simple linear regression model. In general, linear regression models are quite simple, which is a fact that makes them attractive to many users in various domains (Johannesen et al., 2019; Gorucu and Gumrah, 2004). Machine learning algorithms are very useful in building sectors for many applications (Hong et al., 2020).

The models used in time series data productions can be classified under four main categories: regression models including Auto-Regressive Integrated Moving Average (ARIMA) with SARIMA as its seasonal component, artificial neural network approaches, numerical weather prediction models, as well as hybrid models. SARIMA predicts time-series data based on the data's past values. Many studies in building science have used SARIMA methods to develop models for temperature and time-series weather-related data. These models have been conventionally popular for researchers working with time-series data before the proliferation of more sophisticated machine learning approaches (Han et al., 2021). Although SARIMA models are also relatively easy to implement and typically generate reliable results and predictions, these classical regression models possess limitations concerning assumptions of normality, linearity, and variable dependence. Also, SARIMA models work in the short term and they do not scale well in the longer term (Han et al., 2021). Long short-term memory (LSTM), on the other hand, is an artificial recurrent neural network (RNN) architecture used in the field of deep neural networks (DNNs) learning (Kim et al., 2019). The LSTM allows fewer inputs, requires less computation time, and offers superior performance compared to conventional methods such as SARIMA (Han et al., 2021). For example, A. N. Hernandez and F. A. S. Fiorelli studied the utilization of recurrent neural networks to forecast building energy consumption using solar radiation and local temperature (Neto and Fiorelli, 2008). The method was validated and found to perform similar to or better than conventional methods such as SARIMA.

Bourdeau et al. reported a review on six different data-driven building energy modelling and forecasting techniques which are statistical regressions, k nearest neighbours, decision trees, support vector machines, artificial neural networks (ANN), and two combined approaches. Compared to other forecasting techniques, ANN ranks among the most accurate and applied data-driven methods. The performance

evaluation of different models was based on contrariwise unit-based metrics such as the mean absolute error (MAE), and the root mean squared error (RMSE) (Johannesen et al., 2019; Bourdeau et al., 2019). Nowadays, researchers are considering deep learning (DL) models such as recurrent neural networks (RNN) for prediction because of their capability of predicting future trends with performance. DL models can remember the data throughout the prediction process. Yet, these models take a long time to train the data. Therefore, LSTM and GRU were implemented to solve deep RNN time-consuming challenges during the training process by realizing deep and long-term memory cells (Hossain et al., 2021; G é ron, 2019). Many researchers try to increase the model efficiency by using artificial neural networks to evaluate and forecast time series data (Khotanzad and Elragal, 1999; Khotanzad et al., 2000; Suykens et al., 1996; Tonkovi ć et al., 2009; Tektas, 2010; Gorucu et al., 2004). For example, Suykens et al. predicted gas consumption using neural networks considering different input variables such as temperature, oil price, number of clients, and consumption (Suykens et al., 1996). Ravnik et al. forecast daily natural gas using a sigmoid regression and ANN models (Ravnik et al., 2021). Jung M. H. et al. study discussed the impact of weather files on building performance simulations (Han et al., 2021). They proposed a methodology using gated recurrent units (GRU) to generate synthetic localized weather data that are significantly more accurate and representative of local conditions than standard weather files. The predictions were validated against actual on-site measurements, and (GRU) performed best with a low mean squared error achieved, a low mean square error of 2.96 and over 185% improvement in validation accuracy. In their study, Nishimwe and Reiter predicted regional heating degree-days (HDD) trend of −11.76% and cooling degree-days (CDD) of 14.04% for the same period from 2012 to 2050 based on the gated recurrent unit (GRU) an implemented deep learning (DL) model (Nishimwe and Reiter, 2021a). In this paper, monthly maximum and minimum temperatures are forecasted, hence estimating HDD and HC up to 2030, 2040, and 2050 horizons.

Years ago, some studies implemented statistical methods and machine learning (ML) models like ARIMA/SARIMA models (Seasonal Auto-Regressive Integrated Moving Average) to forecast their data (Nury et al., 2013; Box and Jenkins, 1976; Balyani et al., 2012; Anitha Kumari et al., 2014; Khedhiri, 2016; Liu and Lin, 1991; Durmayaz et al., 2000; Maggio and Cacciola, 2009; Monsell, 2007; Karim, 2014; Murat et al., 2018; Wang and Lu, 2006; Ibrahim et al., 2009; Kumar and Jain, 2010; Koch and Sun, 1999; El-Mallah and Elsharkawy, 2016). Most of them mainly considered these models for weekly, monthly, or yearly time series (Khedhiri, 2016; Liu and Lin, 1991; Durmayaz et al., 2000; Maggio and Cacciola, 2009; Erdogdu, 2010). Different methodologies found in literature forecasted time series data, for example, Hyndman and Khandakar generated automatic forecast time series using R (Hyndman and Khandakar, 2008). Several combined forecasting horizons are also reported in the literature, where the authors predicted data on seasonal (Timmer and Lamb, 2007), monthly (using neural networks model) (Suykens et al., 1996), weekly (Khotanzad and Elragal, 1999; Khotanzad et al., 2000; Thaler et al., 2005; Dombayci, 2010), or daily (Ravnik et al., 2021) time intervals. However, the SARIMA model does not tend to give good results for the time series (Murat et al., 2018). Yamak et al. compared ARIMA, LSTM, and GRU models for time series forecasting. They found that based on the MAPE (mean absolute percentage error), the ARIMA model gave the best results, the GRU model worked better than LSTM, however, their study was based on bitcoin's prices data and not temperature data (Yamak et al., 2019). In their study, Makridakis et al. assessed the performance of different classical ML (machine learning) techniques for several forecasting horizons (Makridakis et al., 2018). They evaluated ARIMA and ETS, and based on the MASE (Mean Absolute Scaled Error), ARIMA and ETS performed well compared to other methods such as LSTM and RNN (Recurrent Neural Network). However, they did not evaluate SARIMA and GRU. Aghelpour et al. estimated the monthly temperature forecast in Iran's climate using 3 models namely SARIMA, SVR (Support Vector Regression), and SVR-FA (SVR- Firefly Optimization Algorithm). They found that SARIMA gave a pertinent performance in one climate zone. Other models performed well as well (Aghelpour et al., 2019). In the United States, Valipour used ARIMA and SARIMA for a long-term runoff forecast where SARIMA exceeded ARIMA. However, the author did not consider other DL (deep learning) models to compare with the SARIMA model (Valipour, 2015). Moeeni and Bonakdari forecasted monthly dam reservoir inflow using hybrid SARIMA and ANN models. SARIMA outperformed the other models and the hybrid model diminished the forecast error. However, they did not consider LSTM or GRU in their study (Moeeni and Bonakdari, 2017). On the other hand, Chung et al. compared LSTM and GRU on speech and music signals, where GRU outperformed other RNN models (Chung et al., 2014). Further, Nam et al. forecasted renewable energy scenarios using DL models by comparing them. In their study, they found that GRU gave the best prediction performance (Nam et al., 2020). The models above found in the literature, are necessary for the energy management on a city, a region, or a country scale. For example, Paiho et al. reviewed the impact of new technologies on energy demand management and concluded that the models increase the flexibility of electricity and heat systems (Paiho et al., 2018). In our case study, the models implemented will help with energy management on a regional scale.

Based on different backgrounds and literature reviews, it is hard to tell a user which kind of model to choose for a good prediction unless the users have the same kind of data as a previous user to replicate the same model. Nevertheless, the GRU model performs well in most cases (Hossain et al., 2021; Wang et al., 2021). In this study, the authors have chosen to evaluate and compare 3 AI models which are an ML model SARIMA and DL-based models LSTM and GRU, to choose the best performing model for monthly temperature forecast. This methodology can be replicated elsewhere with the same kind of data.

Furthermore, the heating degree-days (HDD) are accurately calculated using the meteorological equation method, which considers the outside daily average maximum and minimum temperature (Liang et al., 2022) concerning the base temperature (Day and Karayiannis, 1998). This is the standard method for HDD calculation. The base temperature of 15°C is mostly used in Belgium (RMI, 2021). Given the weather in our study area (Wallonia Region of Belgium), the comfort temperature in buildings is 18°C: the base temperature is mostly set to 15°C and the additional 3°C comes from internal (persons, appliances, cooking, etc.) and solar gains. Thus the Royal Meteorological Institute (RMI) of Belgium recommends using the base temperature of 15°C (Moustris et al., 2011; Fleiter et al., 2016). The degree-days (DD) are presented as yearly, monthly, as well as weekly, or on a daily interval. The Annual HDD values are computed as the cumulated sum of daily, weekly, or monthly HDD values for the heating season. In general, for European countries, this heating period is defined as 6 months from 1 October to 31 March. However, the heating season can last longer in northern Europe than in southern Europe (Spinoni et al., 2018). Thus, heating zonation based on each country's laws on heating can be applied. Spinoni et al. (2018) applied the UK Met Office equations for computing the daily HDD: the calculations of the HDD were based on a comparison of daily minimum and maximum air temperatures with the selected base temperature.

The HDD are often used as a climatic measure in building energy calculations (Spinoni et al., 2018). Matzarakis and colleagues explained that the HDD derives from daily air temperature observations and reflects the energy requirements to heat a home, business, or other issues. They concluded that there is an increase in air temperature over the years, resulting in a lower number of heating days, degree days, and heating energy consumption, which may be reduced between 18 and 28 % from 1961 to 2100 (Matzarakis et al., 2009). In the residential sector, space heating constitutes the biggest share of energy consumption amounting to above 80% in colder climates (European Commission, 2016). The share of hot water use in buildings is 25% of total heat consumption in the residential sector and 14% in the tertiary sector. The

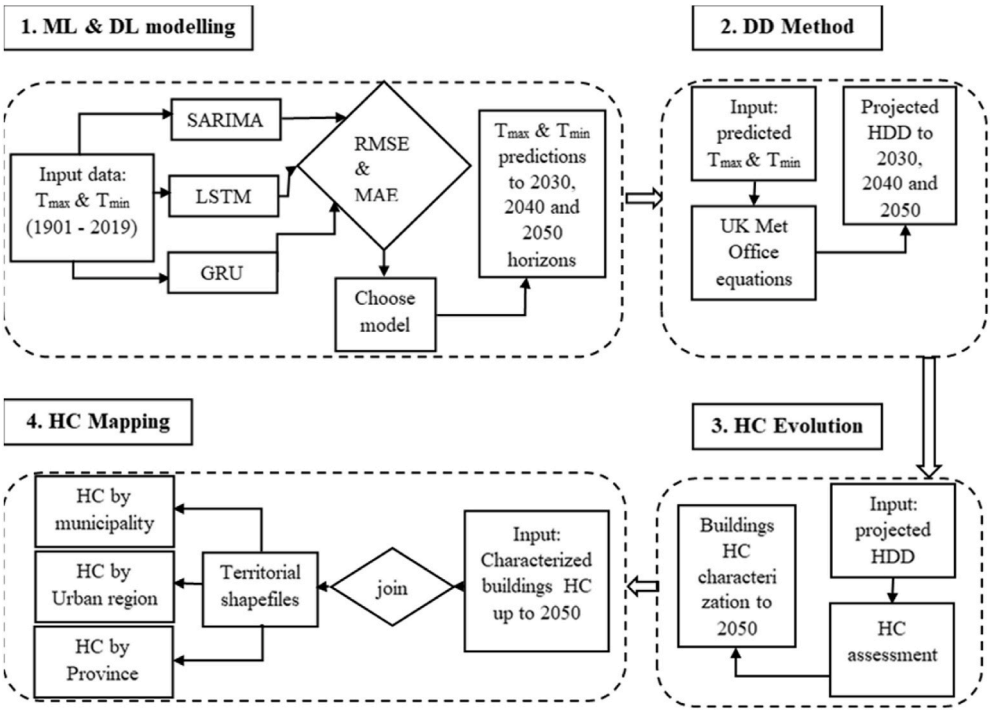

Fig. 1. Summary of combined methodology to estimate the evolution of buildings heat consumption on different horizons namely 2030, 2040, and 2050.

European commission projected a decrease in hot water consumption under European Union (EU) decarbonisation scenarios (European Commission, 2016), but other studies projected on the contrary that hot water consumption would remain stable in the future decades at around the same level as today. Heat consumption data collected in EU countries in the industrial sector showed a distribution of HC for space heating of 85% and HC for water heating of 15% in many European countries (Fleiter et al., 2016).

Spinoni et al. investigated the impact of climate change on the energy demand for heating buildings (Spinoni et al., 2018). For this purpose, the evolution of the HDD indicator has been analysed based on both European climate scenarios RCP4.5 and RCP8.5 emission pathways until the end of the 21st century. The RCP4.5 simulation is moderate and considers that the greenhouse gas (GHG) emissions will peak around the early 2050s and then stabilize, causing a CO_2 equivalent of about 650 ppm (parts per million) and a temperature increase of approximately 1.8–2.0 °C in 2100. On the other hand, RCP8.5 is more extreme and predicts a continuous rise of GHG emissions until 2100, causing a CO_2 equivalent larger than 1370 ppm and a temperature increase close to 4 °C. They showed that for northern Europe, the projected HDD was reducing, ranging from −17 to −23% under RCP4.5, and −21 to −28% under RCP8.5. For central Europe, on the other hand, they showed more homogeneous spatial patterns, and the reduction in HDD was about −18% under RCP4.5 and −22% under RCP8.5 (Spinoni et al., 2015, 2018).

The degree-day (DD) method has been widely used in energy consumption (Durmayaz et al., 2000; Sarak and Satman, 2003). Degree-hours, DD, degree-months, or degree-years are often used as helpful parameters in forecasting energy consumption (RMI, 2021; Ibrahim et al., 2009; Koch and Sun, 1999; Chung et al., 2014; Nam et al., 2020; Paiho et al., 2018; Wang et al., 2021). Other researchers also focused on the degree-hour or DD calculation methods to compute the HDD (Anitha Kumari et al., 2014; Durmayaz et al., 2000; Sarak and Satman, 2003). The forecasting of energy consumption was investigated on regional scales, in cities, and even on individual building scales (Sarak and Satman, 2003).

Throughout this literature review, this paper is aiming at answering the following questions:

(1) How to forecast temperature data to different horizons? The time series analysis such as temperature series analysis can be predicted using different AI models, to select the best performing model for the forecast.
(2) Can HDD data forecast be estimated using temperature data? The HDD is affected by the temperature changes and the base temperature for building comfort.
(3) Could the HC forecast of Wallonia building stock be estimated based on the HDD calculation method? The proposed methodologies from the literature review can also be applied to Wallonia cadastral energy data to forecast the HC.

Many references in the literature studying impacts of climate change on HC of buildings treat the subject by focusing merely on historical HC data and forecast but ignoring the effect of climate change on temperature and HDD (Sarak and Satman, 2003). The authors in this research lay down reproducible methods for HC forecast starting from raw temperature data. Moreover, regarding the temperature forecast, the seasonality of the observed temperature data is exploited using 3 AI models to produce more realistic predicted temperature values. In the first modelling using SARIMA, the authors avoided the linear pattern that characterizes predicted values resulting from simple ARIMA models and linear regression models, often used in the literature. For example, El-Allah and Elsharkawy used ARIMA (3-1-2) and ARIMA (3-2-3) models to carry out short-term predictions, from 2010 to 2020, of annual surface air temperatures in Libya (Tektas, 2010). They did not consider the seasonality of the temperature, leading to a higher maximum absolute percentage error of 4.8%, which may be reduced for example by applying SARIMA models. However, in the second and third modelling, our study used more modern RNN units specifically LSTM and GRU. Finally, the mapping of the HC of the studied building stock is performed considering the whole Wallonia region on 3 scales (municipality, urban region, and province), and not on building scale as found in some previous studies.

The estimation and evolution of energy use in buildings, relative to

climate change, require local temperature data. Thus, the accuracy of HDD calculations depends on the quality and resolution of the temperature change data at the building scale. Although the Global Climate Models (GCMs) such as the Coupled Model Intercomparison Project (CMIP5 and CMIP6) can provide historical and projected temperature data, these models have limited resolution and give better results at large scale (>2000 km) (Kamruzzaman et al., 2021). Moreover, the increase in complexity of these models is a source of biases during climate parameters prediction. This research presents the simplest method for assessing the future impact of the calculated HDD from the predicted temperature at a local scale using historical temperature data.

The innovation key of our study is predicting future HC starting from the temperature data, then mapping the predicted HC on different territorial scales. As the longer historical data of the HC were not available for our case study, this study is helpful to other scientists wanting to predict the HC, based on the temperature historical data, without HC historical data. The results of these predictions are useful for urban planners and decision-makers in terms of sustainable energy management of a region or a country.

3. Methodology

This study used a combination of scientific and calculation methods: the first one is AI modelling which is ML modelling: SARIMA and DL modelling: LSTM and GRU for maximum and minimum temperature predictions. This study analyses the use of three models namely SARIMA, LSTM, and GRU which are currently the leading models in the use of artificial intelligence models for predictions, and proposes a methodology to generate highly accurate localized temperature predictions, suitable for building stock energy consumption simulation applications. The study also compares the performance of these models and validated the GRU model for its outperforming results compared to SARIMA and LSTM models.

The second method consists of applying the UK Met office equations for HDD calculation using forecast temperatures and considering the base temperature of 15°C, mostly used in our case study, Belgium's south part. The third is the degree days method for HC calculation using the HDD forecast values, and finally visualization of the HC spatial distribution by mapping the current HC of residential, tertiary, and industrial buildings and their projected 2050 scenarios. The three prediction models will be compared on their production results and evaluated by calculating the mean absolute error (MAE) and the root mean square error (RMSE) values between real and test data. The 4 used methods are explained below as well as the description of the case study, which consists of the Walloon building stock (Belgium), in a temperate climate in the northern part of Europe. The proposed methodology is summarized in Fig. 1.

3.1. Data preparation

Python programming is used for the time series analysis (TSA) and forecast method considering the monthly maximum (T_{max}) and minimum (T_{min}) temperature data from 1901 to 2019 collected in Belgium by the "Royal Meteorological Institute" (RMI). The daily temperature data are available on the official website of the National Oceanic and Atmospheric Administration (NOAA) (NOAA, 2020). In this study, however, this data is aggregated to monthly temperature data. Next, the temperature data is loaded in RClimdex (1.0) to be cleaned by finding the unreasonable values such as $T_{min} > T_{max}$ (see Table 3). The python software is used for the execution of AI models processes.

3.2. ML modelling: SARIMA

SARIMA (*p, d, q*) (*P, D, Q*)*s* combines three mathematical models:

- auto-regressive (*AR*): *p*
- integrated (*I*): *d*
- and moving-average (*MA*): *q*

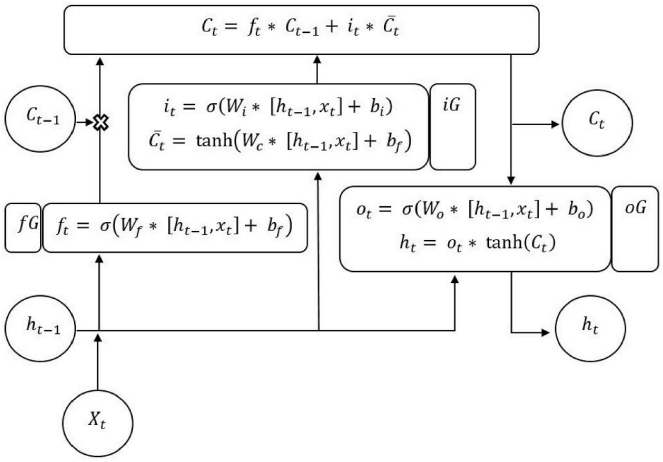

Fig. 2. LSTM model flowchart.

The (*P, D, Q*)*s* are the seasonal components of SARIMA and *s* is the number of periods in the season. Firstly, the monthly temperature series are differenced *d*-times to make them stationary. Secondly, the monthly temperature values from the stationary process (T_x) are modelled by including auto-regressive terms *p*:

$$T_x = c + \sum_{i=1}^{p} \varphi_i t_{x-i} + \varepsilon_x \tag{1}$$

Where: *c* is the constant coefficient, φ_i represents autoregressive coefficients, t_x is the monthly average T_{max} or T_{min} at month *x* and ε_x stands for the error term. Thirdly, *q* is the moving-average term that takes into account previous errors in temperature observations.

$$T_x = \varepsilon_x + \sum_{j=0}^{q} \theta_j \varepsilon_{x-j} \tag{2}$$

Where: θ_j is the moving average coefficient and ε_x is the error term at month *x*.

Finally, by combining these three models (differenced or integrated, auto-regressive, and moving-average), we get the ARIMA model. The form of SARIMA *(p, d, q) (P, D, Q)s* model used can be written in backshift notation as:

$$\varphi_{AR}(B)\varphi_{SAR}(B^S)(1-B)^d(1-B^S)^D T_x = \theta_{MA}(B)\theta_{SMA}(B^S)\varepsilon_x \ldots \tag{3}$$

Where:

- φ_{AR} = non-seasonal AR- parameter,
- θ_{MA} = non-seasonal MA- parameter,
- φ_{SAR} = seasonal AR-parameter,
- θ_{SMA} = seasonal moving average parameter,
- and B = backward shift operator.

The backward operator B is defined as:

$$B_k(T_x) = T_{x-k} \quad x \quad > k;\ x,\ k\epsilon N \tag{4}$$

Where: *k* is the index denoting how many times backward operator *B* is applied to time series T_x characterized by the time interval *x*, and the total number *N* of time intervals.

3.3. DL modelling: LSTM

Fig. 2 illustrates the LSTM model flowchart at the cell state *t* which is

Table 1
Components of LSTM cell.

Component	Representation	Nature	Description
Forget Gate	*fG*	NN with sigmoid	Control what to put in the cell state from short term memory and input *Tmax & Tmin*
Input Gate	*iG*	NN with sigmoid and tanh	Adds input to short term memory
Output Gate	*oG*	NN with sigmoid and tanh	Produces output short term memory for the next cell state C_{t+1}
Hidden state	*H*	Vector	Short term memory
Memory state	*C*	Vector	Long term memory

Table 2
UK Met Office equations (Spinoni et al., 2018) were applied to the computation of the monthly HDD using the monthly maximum and minimum temperatures, the average monthly temperature, and the base temperature.

Case	Weather	Condition	HDD =
1	Uniformly cold month	$T_{max} \leq T_{base}$	$(T_{base} - T_{avg})$ *(7)*
2	Mostly cold month	$T_{avg} \leq T_{base} < T_{max}$	$[(T_{base} - T_{min})/2] - [(T_{max} - T_{base})/4]$ *(8)*
3	Mostly warm month	$T_{min} < T_{base} < T_{avg}$	$(T_{base} - T_{min})/4$ *(9)*
4	Uniformly warm month	$T_{min} \geq T_{base}$	0 (No heating is required)

the present or current state. The parameter X_t is the current input temperature (*Tmax & Tmin*), C_{t-1} and C_t are previous and current memory states with their previous (h_{t-1}) and current (h_t) hidden state respectively, W_f is the weight at forget gate (*fG*), W_i and W_c are the weights at current input gate (*iG*) and W_o the weight at output gate (*oG*). The tanh and sigmoid (σ) are activation functions.

Table 1 summarizes the main components of the LSTM cell.

Input data transformations were performed on T_{max} and T_{min} using the sigmoid and tanh activation functions. Temperature data are fed in the model by a segment of 12 months at any step (current input $X_t = 12$ months), i.e., the model looks back 12 months to predict one month forward (the thirteen-month).

The forget Gate (*fG*) controls how much of the memory is kept. After receiving the input temperature data, the *fG* runs the f_t calculation using the sigmoid function (σ), whose results will ultimately affect the long-term memory called cell state (C: …, C_{t-1}, C_t, C_{t-1}, …). The weights (W: W_f, W_i, W_c, W_o) values are calculated during the training step of the model. The weight assigns estimated values to information that should affect the current cell state.

Next, the model decides through the Input Gate (*iG*) which temperature information from hidden state h_{t-1} and the input X_t will be recorded in the long-term memory (C). The input gate values are calculated through sigmoid activation σ and are transformed to falls between 0 and 1. Next, the *iG* scales the input between −1 and 1 using tanh activation. Finally, the new cell state C_t is estimated by adding both results. The output gate (*oG*) layer is calculated using the temperature input at any step t (e.g., X_t for the current state) and hidden state h_{t-1} of the last step. It is important to notice that the obtained current hidden state (h_t) and current cell state (C_t) will be used in the next step (t+1) as h_{t-1} and C_{t-1} respectively.

Finally, the result C_t is stored as the new long-term memory (cell state) which keeps the long-term memory updated.

3.4. DL modelling: GRU

GRU model is almost similar to LSTM except that it has two gates: reset gate (*rG*) and update gate (*uG*). GRU does not use the memory unit to control the flow of information like the LSTM. It directly makes use of the all-hidden states without any control.

The *rG* determines how to combine new input (*Tmax & Tmin*) to previous memory (h_{t-1}) running the sigmoid function σ to calculate r_t. *uG* determines how much of the previous state to keep by calculating z_t. The *uG* in GRU is what the input gate and forget gate were in LSTM.

As shown above in Fig. 3, both state vectors (h_t and $\widetilde{h_t}$) are merged into a single vector h_t. There is no output gate; the full state vector is output at every time step.

3.5. Models evaluation

To evaluate the performance of the models, the root mean squared error (RMSE) and mean absolute error (MAE) are defined respectively by the formulas:

$$RMSE = \sqrt{\frac{1}{n}\sum_{x=1}^{n}\varepsilon_x^2} \quad (5)$$

And,

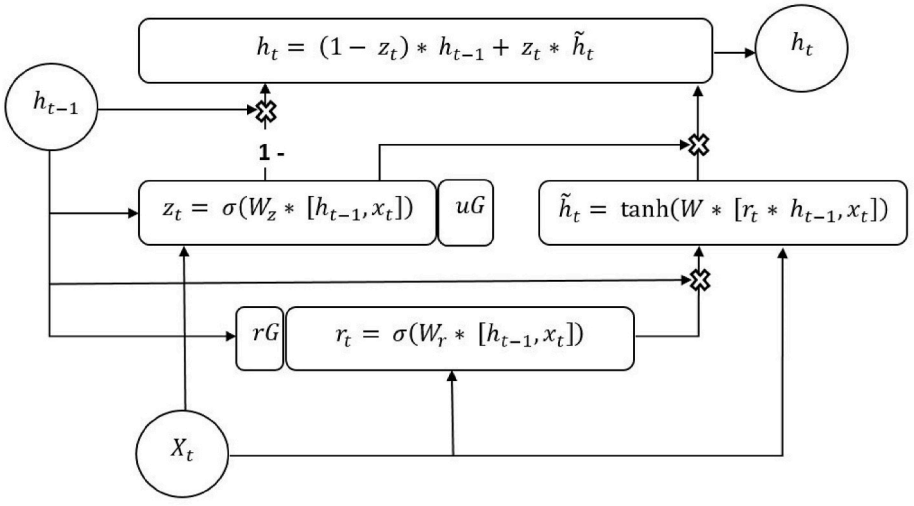

Fig. 3. GRU model flowchart at the cell state t. Wr is the weight at reset gate (rG), Wz is the weight at update gate (uG), and Wt is the weight cell state vector ($\widetilde{h_t}$).

Table 3
Temperature observation errors: Tmax is lower than Tmin. The RClimdex (1.0) package of the R software was used for Tmax and Tmin observation errors identification.

Year	Month	Day	T_{max}	T_{min}	T_{max}-T_{min}
1941	1	1	−2.9	−2.8	−0.1
1944	1	10	5.1	7.2	−2.1
1978	5	2	9.6	9.9	−0.3
1981	12	15	−1.9	−1.8	−0.1

Table 4
Models evaluations: T_{max} and T_{min} RMSE and MAE.

Period	Errors	SARIMA		LSTM		GRU	
		T_{max}	T_{min}	T_{max}	T_{min}	T_{max}	T_{min}
2020–2030	MAE	1.44	1.17	1.43	0.97	**1.21**	**0.81**
	RMSE	1.81	1.48	1.77	1.2	**1.46**	**1.01**
2020–2040	MAE	1.41	1.18	1.44	1.01	**1.29**	**0.9**
	RMSE	1.79	1.48	1.72	1.26	**1.6**	**1.12**
2020–2050	MAE	1.45	1.22	1.58	1.11	**1.42**	**1.01**
	RMSE	1.83	1.54	1.88	1.39	**1.77**	**1.25**

$$MAE = \frac{1}{n}\sum_{x=1}^{n}\left|\varepsilon_x\right| \tag{6}$$

Where n is the number of periods and $\varepsilon_x = t_x - \hat{t_x}$ is the predicted error between the temperature actual value t_x and the predicted value $\hat{t_x}$. The smaller the RMSE or MAE values, the better is the model. See Table 4 for the results from the models' evaluation.

The data are split into train and test sets. The test set is equal to the forecasting set which corresponds to thirty-one years for this study. This forecasting period is divided into three sets: for 11 first years to get the forecasting horizon of 2030, next, another 10 years for the 2040 horizon, and finally another 10 years for the 2050 horizon. On the other hand, the train set is the remaining data. AI models are fitted on the train set, then evaluated on the test set to check for model accuracy. The models are refitted on the entire data set for predictions. Finally, the temperature data are forecasted first for horizon 2030, next for 2040, and then next for 2050.

3.6. HDD calculation

The UK Met Office equations method is used to calculate the monthly HDD. The following table explains how the HDD are calculated based on temperature data.

In this table, T_{base} (15 °C) is the fixed base temperature, T_{max} and T_{min} are the outside forecast average maximum and minimum temperatures given by SARIMA, LSTM, and GRU models, and T_{avg} is the monthly average temperature. The HDD is calculated using the forecast temperature data. The formula for HDD calculation is applied related to the conditions specified in Table 2. The months are categorized into four different cases related to the weather conditions.

3.7. HC estimation

The degree-day method is applied to forecast the estimation of the building heating consumption (*HC*) using previously obtained *HDD* values.

For residential buildings:

$$HC_{y,r} = \left(0.75 * HC_{ref,r}\right) * \left(HDD_y/\mathrm{HDD_{ref}}\right) + \left(0.25 * \mathrm{HC_{ref,r}}\right) \tag{10}$$

Where: $HC_{ref,r}$, and HDD_{ref} are respectively referencing annual values of *HC* and *HDD* for the year 2012, and $HC_{y,r}$, and HDD_y are present annual

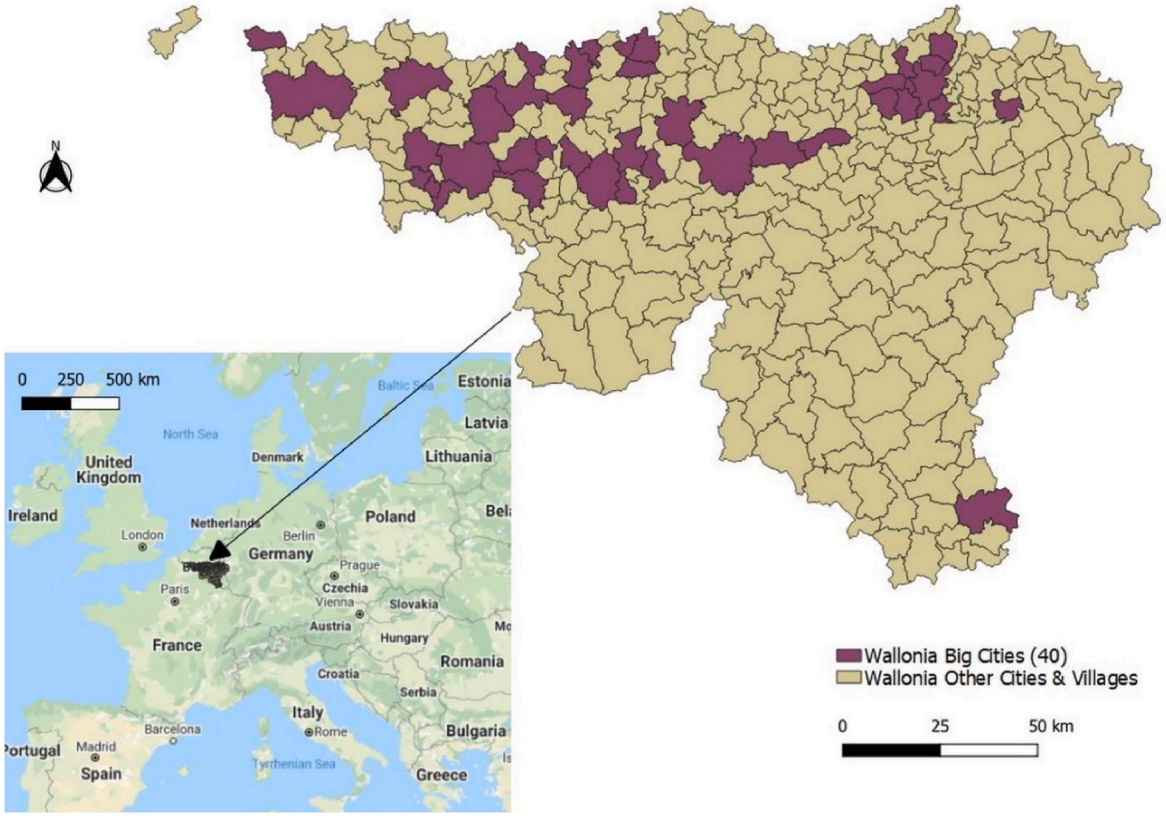

Fig. 4. *Wallonia's geographic situation in Europe and presentation of Wallonia's 40 big cities. Wallonia is the southern region and French-speaking part of Belgium, including 262 cities and municipalities. (Source* (Nishimwe and Reiter, 2021b)*:).*

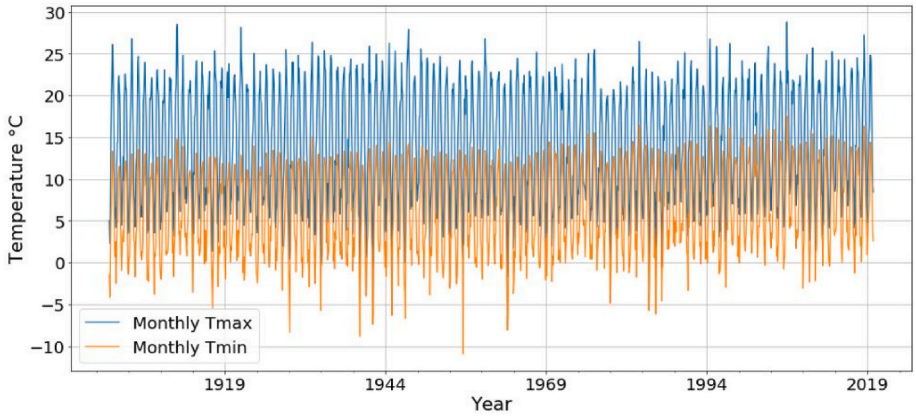

Fig. 5. Monthly maximum (Tmax) and minimum (Tmin) temperature data from 1901 to 2019. These are national data collected in Belgium by the RMI. They are available on the official website of the NOAA (Day and Karayiannis, 1998).

values of *HC* and *HDD* respectively. The correction factor of 0.75 corresponds to 75% of heating consumption and that of 0.25 corresponds to 25% of domestic hot water production.

For tertiary and industrial buildings:

$$HC_{y,t} = (0.85 * HC_{ref,t}) * (HDD_y/\mathrm{HDD_{ref}}) + (0.15 * \mathrm{HC_{ref,t}}) \quad (11)$$

$$HC_{y,i} = (0.85 * HC_{ref,i}) * (HDD_y/\mathrm{HDD_{ref}}) + (0.15 * \mathrm{HC_{ref,i}}) \quad (12)$$

Where: $HC_{ref,t}$, and $HC_{ref,i}$ respectively reference values for tertiary HC for the year 2012 and industrial buildings' HC for the year 2016, and $HC_{y,t}$, and $HC_{y,i}$ are present annual values of HC for tertiary and industrial buildings respectively. For tertiary and industrial sectors, the correction factors of 85% for heating consumption and 15% for the production of domestic hot water are applied. These repartition factors between the heating consumption and domestic hot water production for residential, tertiary and industrial buildings were investigated by Fleiter et al. (2016) and the European Commission (European Commission, 2016) in European countries with cold climates.

3.8. HC mapping

QGIS and Python software are used for mapping. The authors first mapped the residential, tertiary, and industrial buildings HC (Figs. 13–15) on a municipality scale. In QGIS, the natural breaks (Jenks) classification for graduated symbols is applied considering 6 classes for the residential sector, 8 classes for the tertiary sector, and 7 classes for the industrial sector. The Natural breaks of Jenks group better similar data values and optimize the differences between the classes. They reduce the variance within classes and maximize the variance between classes, and consider the natural data trends to classify them. The thresholds are fixed for each building sector (residential, tertiary, or industrial). Whilst fixing the threshold, a significant jump is seen in classes which helped to choose the number of classes for each building sector. This method of classification highlights with colours the spatial distribution of HC classes for 2012/2016 maps and 2050 maps for each building sector. Secondly, the residential, tertiary, and industrial HC are aggregated on urban regions scale and mapped using graduated symbols with natural beaks for classification and also using the diagrams to compare actual and forecast HC for each Wallonia urban region (Fig. 16). Lastly, with python programming, the residential, tertiary, and industrial buildings HC is aggregated based on the structure of the urban area defined by Van Hecke et al. (Van Hecke et al., 2009) for each province. The results are plotted with Python software and then mapped (Fig. 17) on each province in QGIS software.

3.9. Case study

The Belgian Cadastral database has more than 6.6 million buildings (Nishimwe and Reiter, 2021b). In Wallonia, which is the region located in the South part of Belgium (see Fig. 4), the building stock consumes, in terms of annual HC, approximately 29.39 TWh for residential buildings, 11.9 TWh for tertiary buildings, and 34.86 TWh for industrial buildings. Nishimwe and Reiter found that for a 1% increase in the number of existing buildings in a statistical sector (SS), the HC increases by the rate of about 0.93% for the residential sector, 1% for the tertiary sector, and 2.01% for the industrial sector (Nishimwe and Reiter, 2021b). Dense cities and important industrial areas, which mostly are located in the northern part of the Walloon Region, have higher HC in general, compared to the rural areas. The following figure represents the studied region (Wallonia), its main cities, and all its municipalities.

4. Results and discussion

4.1. Data cleaning and preparation

The outdoor maximum and minimum temperature data, in Fig. 5, recorded in Belgium from 1901 to 2019 are used for creating suitable artificial intelligence models.

The identified bias in the temperature data recordings in Table 3 are typical errors that are often committed by the observers during the thermometer reading. The values are shifted between the T_{max} and T_{min} observations of the day when the error was committed as recommended by the National Climate Data Centre (NCDC) in the NOAA user manual (Zhang and Yang, 2004).

4.2. Models evaluation and temperature (Tmax & Tmin) prediction and forecasting

The 3 models implemented are evaluated based on RMSE and MAE for each prediction horizon (2030, 2040, and 2050). Based on the results presented in Table 4, LSTM and GRU perform better than SARIMA, and GRU has the best performance compared to the other models. For this case, the authors have chosen to map the results based on GRU forecast results.

Two approaches were combined to determine the SARIMA parameters: ACF and PACF plots, and the Akaike Information Criterion (AIC) metric. The ACF and PACF plots were used to investigate the temperature data characteristics and then a grid search was used to identify the best parameters. The lower out-of-sample (test data) prediction error (AIC), the more predictive is the SARIMA model. Thus, the chosen SARIMA models for T_{max} and T_{min} are respectively (1, 1, 1) $(0, 1, 1)_{12}$ and (1, 1, 1) $(0, 1, 1)_{12}$. Regarding LSTM and GRU, the used activation

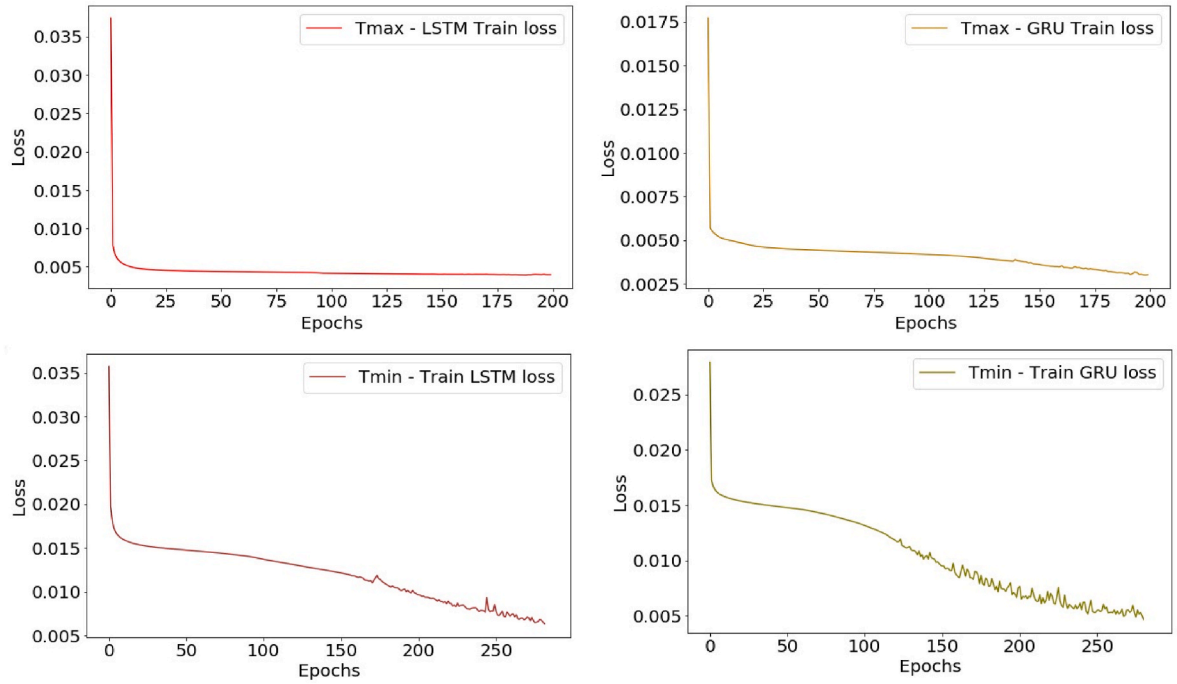

Fig. 6. GRU and LSTM train loss for Tmax and Tmin. The loss is converging to an unchanging value as the epochs increase.

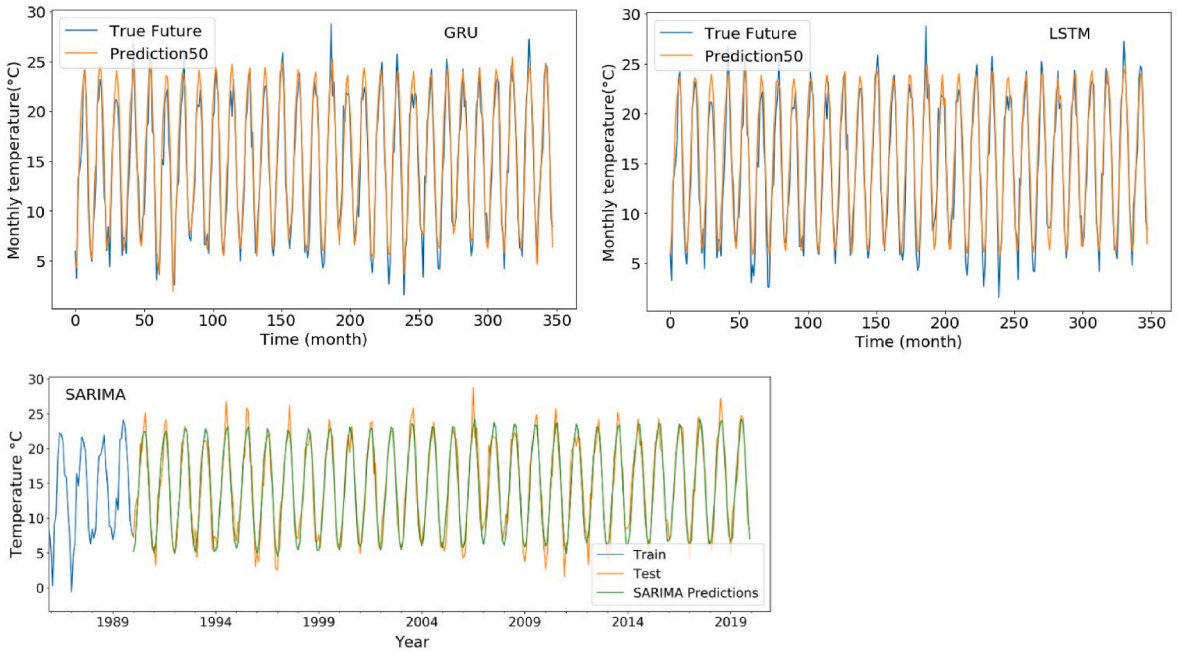

Fig. 7. GRU, LSTM, and SARIMA predictions. For all the 3 models, visually the predictions fit the test sets.

functions used to run the models are sigmoid and tanh, with the optimizer adam.

First, a few epochs were chosen but the loss did not converge. As the models were running, the loss started to converge at 200 epochs, consequently, in this study, the authors stopped at 200 epochs for LSTM and GRU models (see Fig. 6).

Fig. 7 displays the predictions from the 3 models. Throughout the prediction process, it is found that the predictions are fit to the test data for all models. Visually it is hard to tell which is the best model, that is why it is advised to evaluate the models either on RMSE or MAE (see Table 4).

The following 2 figures (Fig. 8 and Fig. 9), illustrate the predictions and forecasts from LSTM and GRU models for T_{max} and T_{min} up to the 2050 horizons. These two models are performing well but visually GRU emphasises more seasonality trends than LSTM.

Moreover, from 2012 to 2050, the authors assessed the temperature increase based on the results from the 3 implemented models. The UN Framework Convention on Climate Change report projects the global temperature increase of 1.5°C by 2100 under scenario RCP2.6 and for the RCP4.5 scenario, the global temperature will surpass 2°C beyond 2100 (UNFCCC, 2015). Table 6 shows the average temperature increase based on 3 models. SARIMA model is overestimating the temperature

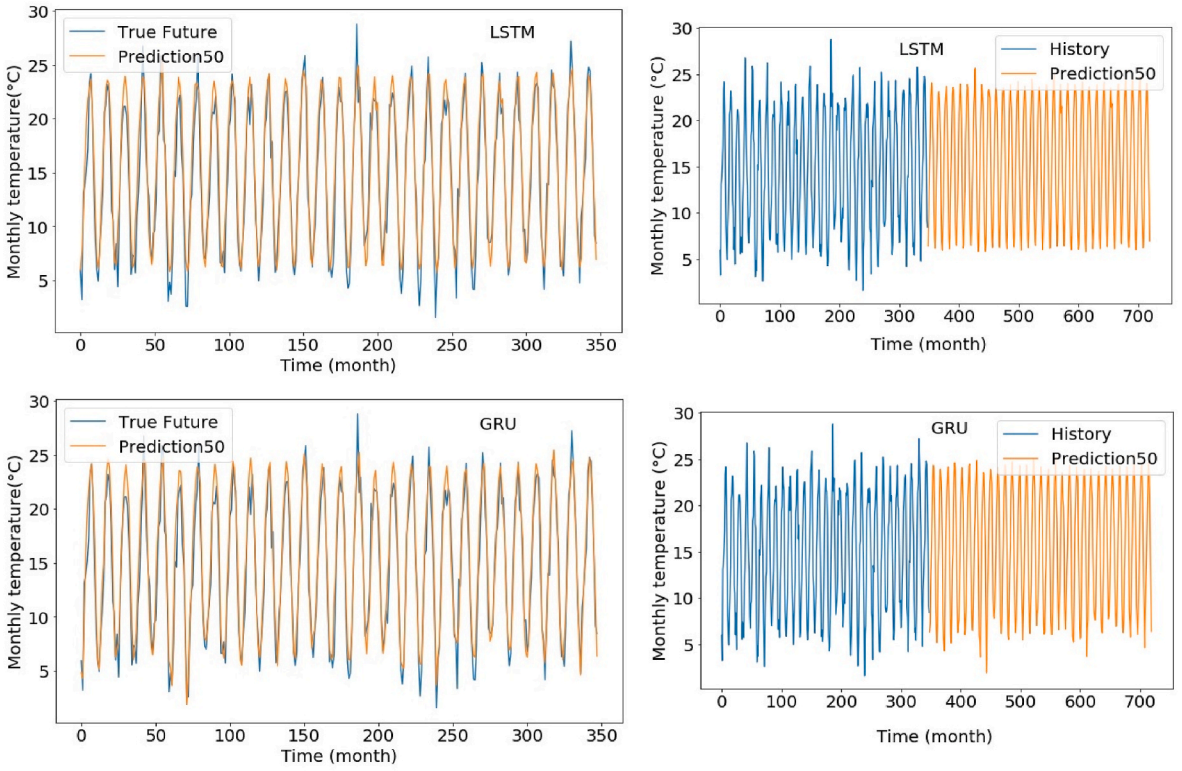

Fig. 8. T_{max} prediction and forecast up to 2050 horizon for LSTM and GRU models.

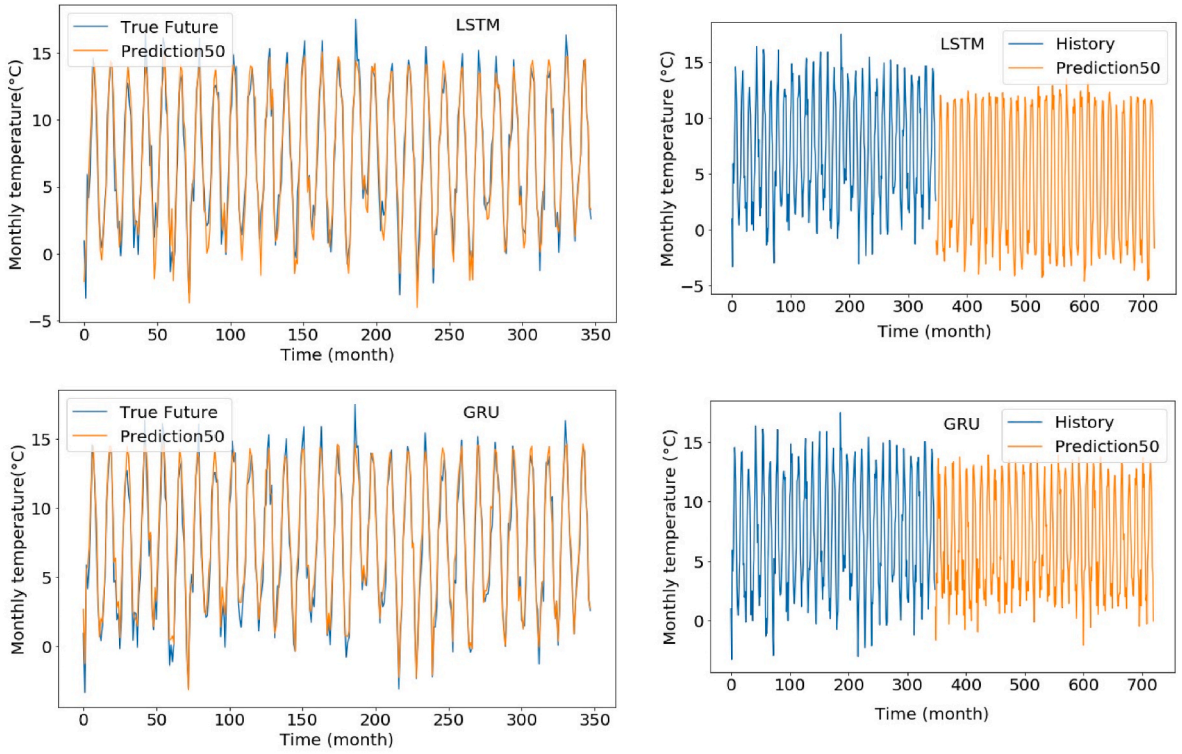

Fig. 9. T_{min} prediction and forecast up to 2050 horizon for LSTM and GRU models.

increase, LSTM is underestimating and GRU is giving more realistic temperature projections.

The average temperature will increase by 0.75°C from 2012 to 2050 if the current human activities don't change. Based on this, the authors used GRU results only for mapping.

Table 5
The heat season's categorization is related to the conditions specified in Table 1. Months are classified by comparing the monthly T_{max} and T_{min} to the base temperature T_{base} and monthly average temperature T_{avg}.

Period	Case	Category	Season
1 November – 31 March	1	Uniformly cold month	Heating season
1 April – 31 May, October	2	Mostly cold month	Heating season
September	3. a	Mostly warm month	Heating season
1 June – 31 August	3. b	Mostly warm month	No heating is required

Table 6
Average temperature increase, average annual HDD and annual average HC (TWh) decrease based on SARIMA, LSTM, and GRU models, for residential, tertiary, and industrial buildings, from 2012 to 2050 for residential and tertiary buildings, and from 2016 to 2050 for industrial buildings.

	SARIMA	LSTM	GRU
Tavg (°C)	10.38% (+ 2.28°C)	4.06% (+ 0.17°C)	5.35% (+ 0.75°C)
HDD	−17.23%	−8.93%	−11.76%
Residential HC (TWh)	−12.92%	−6.70%	−8.82%
Tertiary HC (TWh)	−14.64%	−7.59%	−10.00%
Industrial HC (TWh)	−15.83%	−8.90%	−11.26%

4.3. Heating degree days assessment

In the considered case study, nine months (from 1st September to 31st May) are classified as the heating season for the Belgium region. During that period, from 2020 to 2050, the monthly HDD values vary from 20 to 342 for SARIMA, from 7 to 394 for LSTM, and from 20 to 413 for GRU. However, for June, July, and August, the HDD values are not taken into account, because no heating is required (Table 5).

Furthermore, the comparisons of average temperature and HDD projections and their trends from the 3 executed models are presented in Fig. 10. The GRU model outperformed other models.

The visualization of the above plots show that LSTM and GRU models performed well but not SARIMA which is showing the temperature increase and HDD decrease without considering seasonality trends. The decrease in yearly HDD over the considered case study corresponds to −17.23 % for SARIMA, −8.93% for LSTM, and −11.76% for GRU during the studied period from 2012 to 2050. The results are compared with other European studies for the period from 1981 to 2100. For the near future in northern Europe, they projected a decrease in HDD ranging from −17 to −23 % under RCP4.5 (650 ppm, 9 billion of population and temperature increase between 1.8 and 2.0 °C in 2100), and −21 to −28 % under RCP8.5 scenarios (1370 ppm, 15 billion of population and temperature increase of 4 °C in 2100) (Spinoni et al., 2018). The SARIMA model HDD decrease is close to projected values from the RCP4.5 scenario up to 2100, whereas the LSTM and GRU models HDD decreases are reasonable because our study goes up to 2050. These findings show that the SARIMA model overestimates the HDD reduction in 2050. However, if nothing is done to reduce GHG and thus stop the effect of climate change on the increase of temperature, the decrease in HDD may increase considerably.

4.4. Heat consumption

The energy needed for internal heating is approximately projected inferred from HDD values in this study. Regarding the spatial distribution of HDD in Wallonia, there is a clear decrease in HC related to that pattern. The HC decreases at horizon 2050 for all building types are summarized in Table 6. A study in Germany, which used linear regression, forecasted a decrease in buildings heating energy consumption between −18 and −28% from 1961 to 2100 (Matzarakis et al., 2009), whereas our study gave a decrease in HC of the three building sectors of

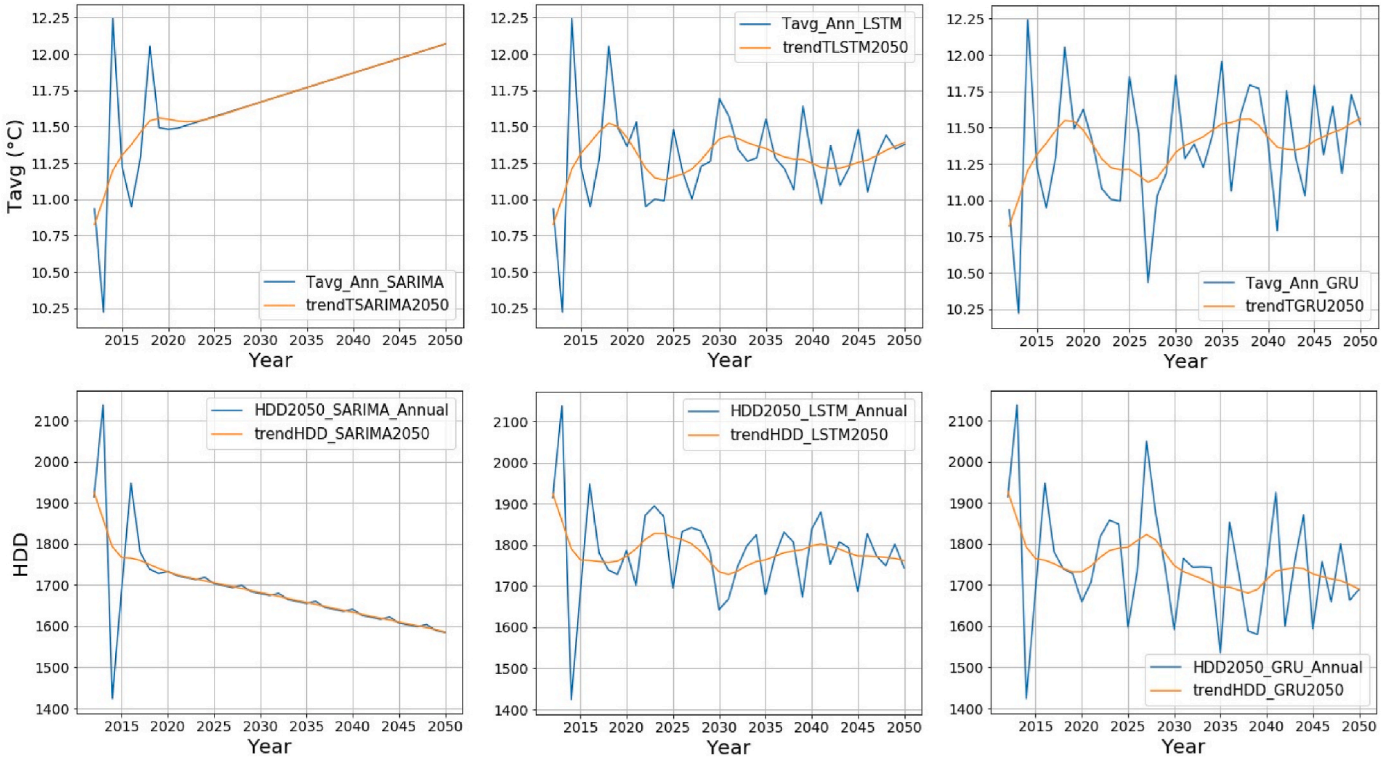

Fig. 10. Average temperature and HDD projections (in blue) and trends (in orange) up to the 2050 horizon. Top: average temperature, bottom: HDD. From left to right: SARIMA, LSTM, and GRU models respectively. (For interpretation of the references to colour in this figure legend, the reader is referred to the Web version of this article.)

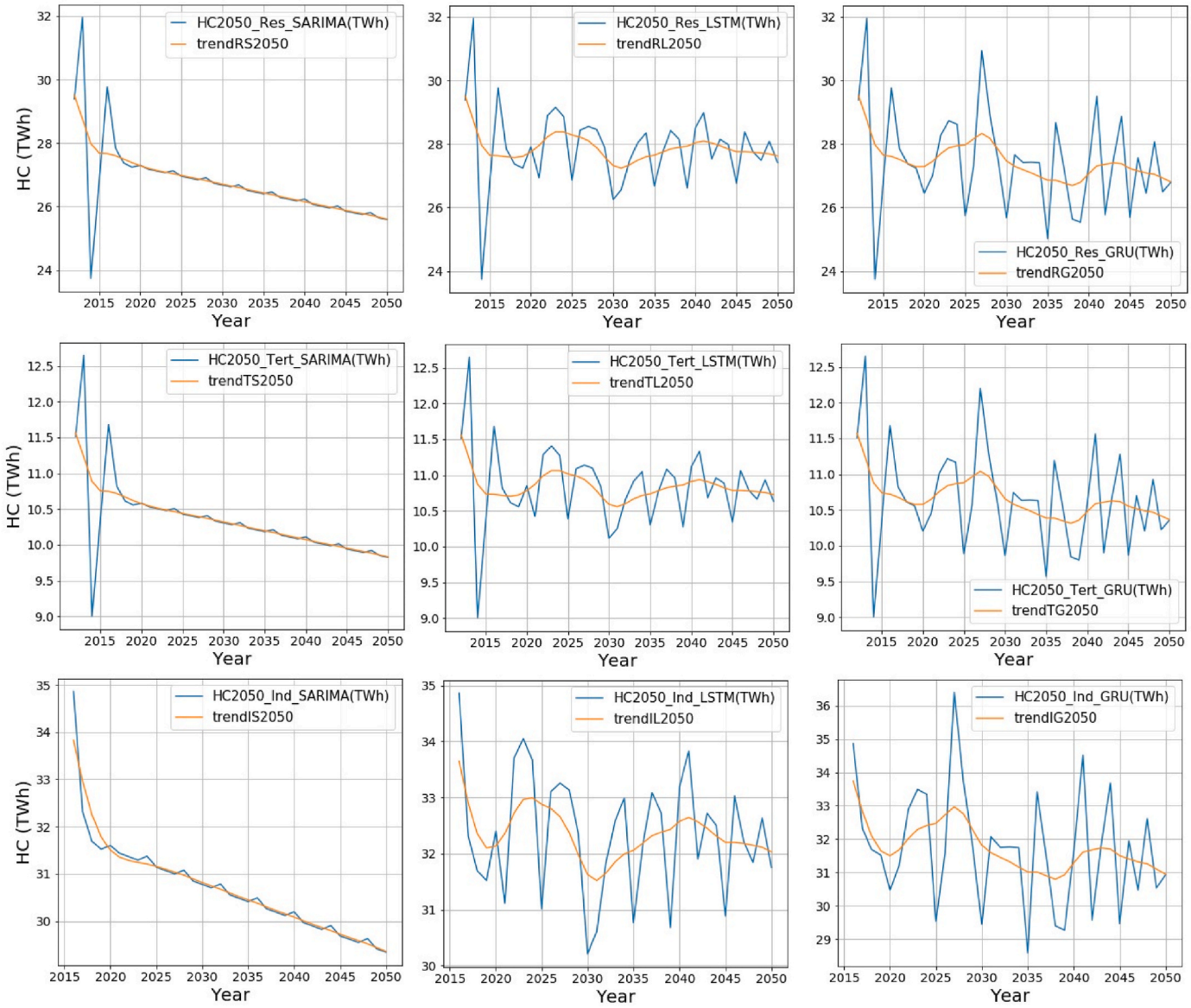

Fig. 11. Yearly average residential, tertiary, and industrial buildings HC projections (blue) and trends (orange) up to 2050 from the SARIMA, LSTM, and GRU modelling. (For interpretation of the references to colour in this figure legend, the reader is referred to the Web version of this article.)

−12.92 to −15.83%, −6.70 to −8.90% and −8.82 to −11.26% for SARIMA, LSTM, and GRU respectively from 2012/2016 to 2050.

In Wallonia (our case study), the HC for industrial and residential buildings is higher compared to the HC for tertiary buildings (Fig. 11). Industrial and residential sectors are key sectors to target to reach the European goals in terms of reduction of the HC in buildings.

The spatial distribution of the forecasted HC for existing residential, tertiary, and industrial buildings in 2050 is presented in Figs. 13–17. For residential buildings, the HC is higher in big cities mainly located in the northern part of the Wallonia Region. The HC of tertiary buildings is more extended in the whole region, while the HC of industrial buildings is concentrated in industrial municipalities, often located on the outskirts of the main Walloon cities. The maps clearly show a decrease in buildings HC from 2012 to 2050 for residential and tertiary buildings and from 2016 to 2050 for industrial buildings.

Fig. 12 presents the building stock HC from 2012/2016 to 2050 based on the chosen model GRU which performed well.

From Figs. 13–15, there are variabilities between classes. For residential buildings, the HC relative difference (RD) from 2012 to 2050 of −8.84% based on the minimum HC value and −8.82% based on the maximum HC value (Fig. 13) on the municipality scale, is similar to the value in Table 7 (a): -8.82% on a regional scale. The reduction of HC from 2012 to 2050 is the same in higher or lower heat-consuming municipalities. Nevertheless, for tertiary buildings in Fig. 14, there are significant irregularities in classes specifically from class 2 to class 5 related to the different tertiary functions existing or not in the municipalities. For example, there is a strong difference in consumption between small tertiary buildings (e.g. shops or schools) and big tertiary buildings (e.g. hospitals or swimming pools). For industrial buildings, however, in Fig. 15, similarities between classes are noticed and the RD of HC reduction from 2016 to 2050 is −11.26% on the municipality scale which is also equal to the value in Table 7 (b): -11.26% on a regional scale.

Fig. 16 illustrates the difference in the aggregated annual HC of residential, tertiary, and industrial buildings in the urban region from 2016 to 2050. As the HC for residential and tertiary buildings have been calculated for 2012 and HC for industrial buildings have been calculated for 2016, the authors used predicted data up to 2016 for residential and tertiary buildings to compare them with the calculated industrial buildings HC for 2016. The reduction of HC, calculated on the sum of HC

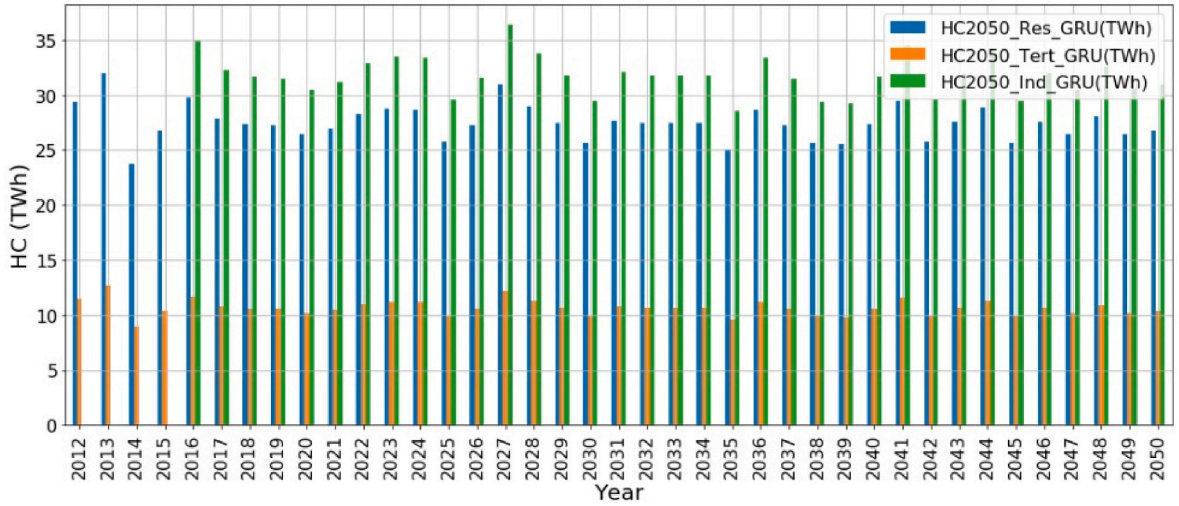

Fig. 12. Total HC for residential (blue), tertiary (orange), and industrial (green) buildings up to 2050 based on GRU projections results. (For interpretation of the references to colour in this figure legend, the reader is referred to the Web version of this article.)

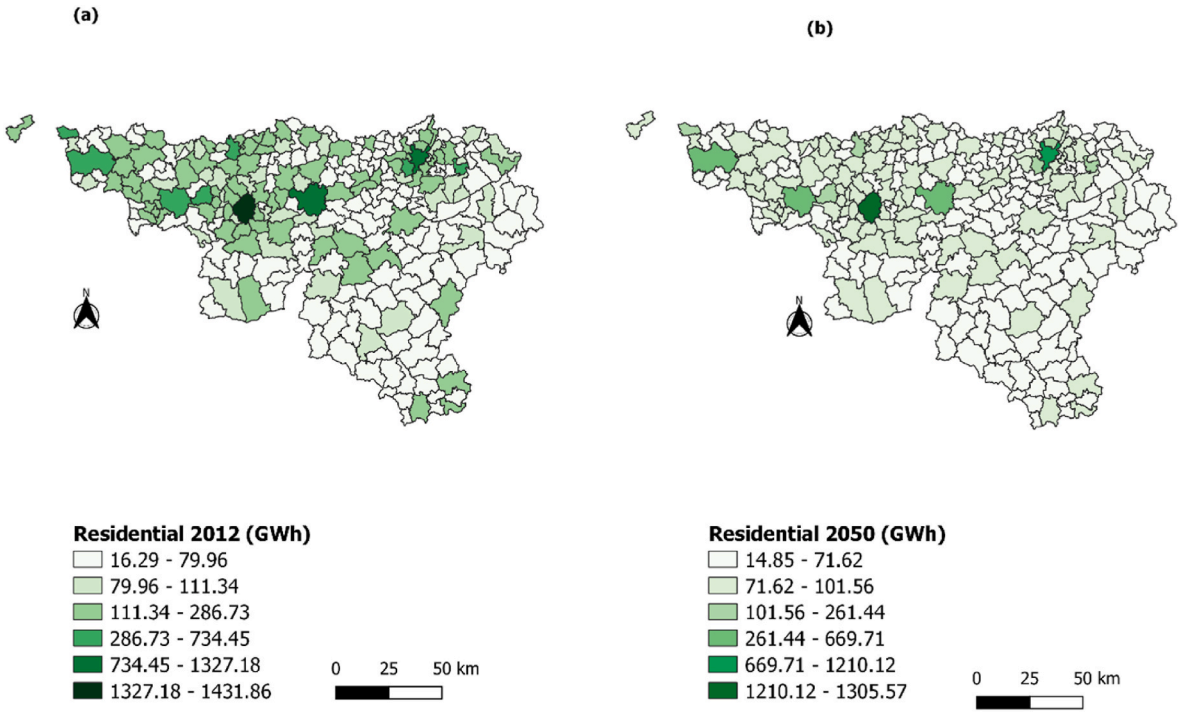

Fig. 13. HC values of 2012 for Wallonia existing residential buildings (a) and forecast HC values of Wallonia existing residential buildings for horizon 2050 (b). The northern part of the Wallonia region with big cities has higher HC values.

of all residential, tertiary, and industrial buildings of each urban region, varies from −10.39 % to −10.91%. The highest reduction of an urban region HC, in Namur urban region, is mainly caused by the highest reduction of industrial buildings HC.

Fig. 17 shows the distribution of annual HC of the aggregated building stock in each province, based on the structure of urban areas defined by Van Hecke et al. (Van Hecke et al., 2009): agglomeration, suburbs, and alternating migrant zones. Where a municipality was not classified in this structure, the authors classified it in other areas, which stand for rural, semi-rural, and low-density peri-urban areas, as well as small cities or villages, regional landscape cities, industrial furrow, and border municipalities with neighbouring countries. The impact of climate change on the HC of the various structures in built-up areas is almost identical regardless of the built morphology or the province. The difference seems negligible: it is less than 0.54% between the different built structures in the same province and it is less than 0.42% between the values obtained for the same built structure in the different provinces.

The residential buildings HC change from 2012 to 2050 varies from −7.01% in 2020 to −8.82% in 2050 and the tertiary buildings HC change varies from −7.94% in 2020 to −10% in 2050, while the change in industrial buildings HC from 2016 to 2050 varies from −9.24% in 2020 to −11.26% in 2050. The industrial buildings have the highest HC values which are obviously related to the larger heated area but also to larger heat loss surfaces of these buildings per volume unit compared to residential and tertiary buildings. Industrial buildings are often less compact than residential and tertiary buildings, which notably include a large number of joined buildings. Thus, at a similar temperature increase

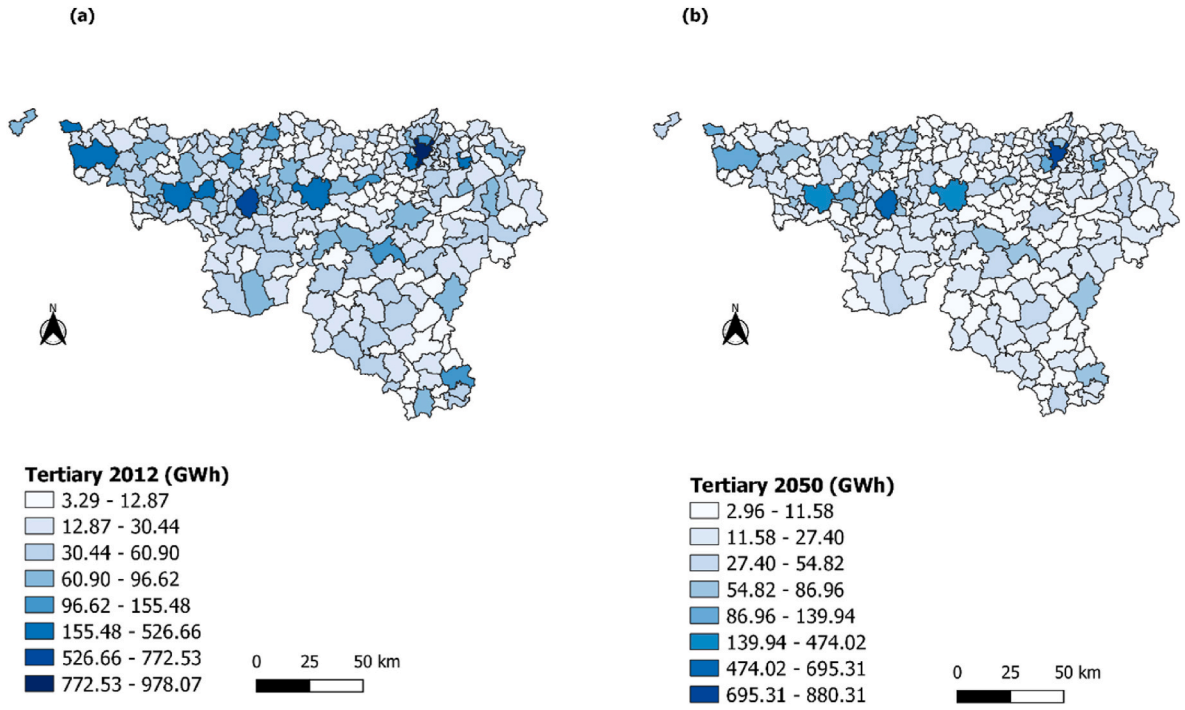

Fig. 14. HC values of 2012 for Wallonia existing tertiary buildings (a) and forecast HC values of Wallonia existing tertiary buildings for horizon 2050 (b). The HC is more distributed to the whole Wallonia region except few cities in the northern part of the region that present higher HC values.

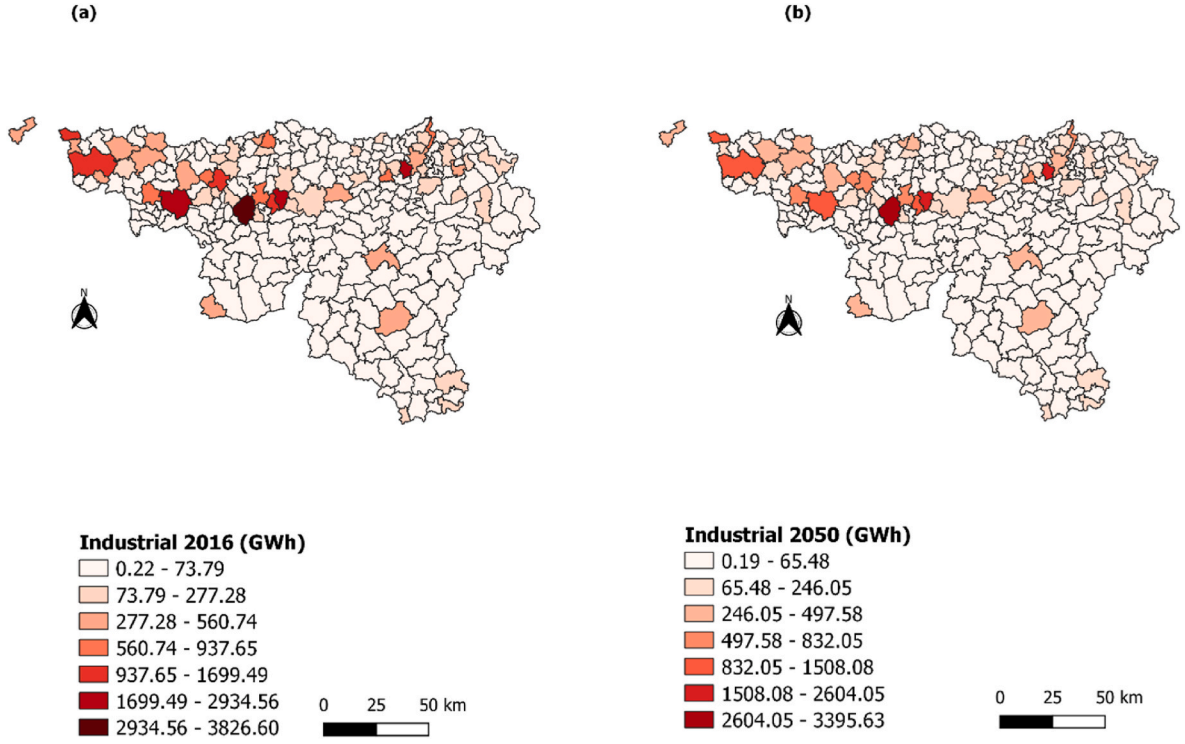

Fig. 15. HC values of 2016 for Wallonia existing industrial buildings (a) and forecast HC values of Wallonia existing industrial buildings for horizon 2050 (b). Nearly all the HC for industrial buildings is located in the northern part of the Wallonia Region, in industrial municipalities, often located on the outskirts of the main cities.

trend, the decrease in the HC rate of the industrial buildings is more significant compared to the HC reduction in residential and tertiary buildings.

5. Limitations of this study

In this research, the authors used historical temperature data to forecast HC. It could be interesting to use historical HC data during the forecast but that data is not available. Moreover, other variables like humidity, precipitation, the behaviour of occupants in the buildings

Table 7
(a) and (b). HC reduction for residential, tertiary, and industrial buildings expressed in %. The existing (original) HC data for residential and tertiary buildings are for the year 2012, while for industrial buildings they are for the year 2016 (Nishimwe and Reiter, 2021b).

(a)			(b)	
Period	Residential	Tertiary	Period	Industrial
2012–2020	−7.01 %	−7.94 %	2016–2020	−9.24 %
2012–2030	−7.64 %	−8.66 %	2016–2030	−10.00 %
2012–2040	−8.50 %	−9.63 %	2016–2040	−10.90 %
2012–2050	−8.82 %	−10.00 %	2016–2050	−11.26 %

(Attia et al., 2022; Almeida et al., 2021), and other exogenous variables (An đ elkovi ć and Bajatovi ć, 2020), as well as influencing weather parameters such as solar heat and wind (Bilous et al., 2018) could be interesting inputs for the models in forecasting the data.

This study did not consider the evolution of the building stock. The main goal of this study was to study the HC evolution of the existing building stock considering the climate data evolution, namely temperature data from 2019 to 2050. But the evolution of the building stock, heating system improvement of buildings, energy efficiency increase of the buildings' envelope thanks to renovations, etc. have to be taken into account for HC estimations in future studies. The impact of energy prices and population income variables on future buildings' HC should also be interesting to study.

6. Conclusion and further research

This article presents a reproducible methodology for HC forecast starting from cadastral data and raw temperature data, combining recognized scientific and calculation methods to produce decision support tools for territorial energy management, and its application in a case study in a temperate climate of the Northern part of Europe. These used scientific and calculation methods are: (1) the forecast of temperature using SARIMA, LSTM, and GRU prediction models, (2) the estimation of HDD using the predicted temperature, (3) the assessment of HC using energy equations applied to residential, tertiary and industrial buildings, and (4) the HC cartography at a regional scale.

The real maximum (T_{max}) and minimum (T_{min}) temperature observations data from 43,464 days in the period between January 1, 1901, and December 31, 2019, have been used in this study. The dataset was cleaned and divided into a training set and a test set. All the observations from January 1, 1901, to December 31, 1989, were used as a training set and the test set includes the remaining data, i.e. from January 1, 1990, to December 31, 2019, which corresponds to thirty years. SARIMA $(1, 1, 1)(0, 1, 1)_{12}$ model was selected, LSTM and GRU models used sigmoid and tnah activation function with adam as an optimizer for T_{max} and T_{min} forecasting. These 3 models are compared on temperature, HDD, and HC predictions and forecasts and then evaluated based on MAE and RMSE to see which model is the best. GRU model performed very well compared to the other models and was chosen as the most appropriate model in this study. All the model predictions of the T_{max} and T_{min} are performed at a 95% confidence interval.

Over the studied period from 2012 to 2050, the yearly HDD in Belgium decreased by −8.82 % for residential, −10.00 % for tertiary, and −11.26 % for industrial buildings HC. The findings show the temperature increases by 5.35% (+0.75°C) and HDD decrease by −11.76% based on GRU modelling from 2012 to 2050. These findings were compared to results found in other European studies. It should be noted that the heating season can last longer in northern Europe than in southern, which justifies the nine months of heating found from the temperature historical data in this study. The temperature will continuously rise beyond the year 2050, consequently, the HC will further decrease.

The respective decreases in HC generally follow the corresponding temperature trends. The geographical factors such as the regional location and the latitude have also a noticeable impact on the building HC (Khedhiri, 2016). Although only the temperature variable was

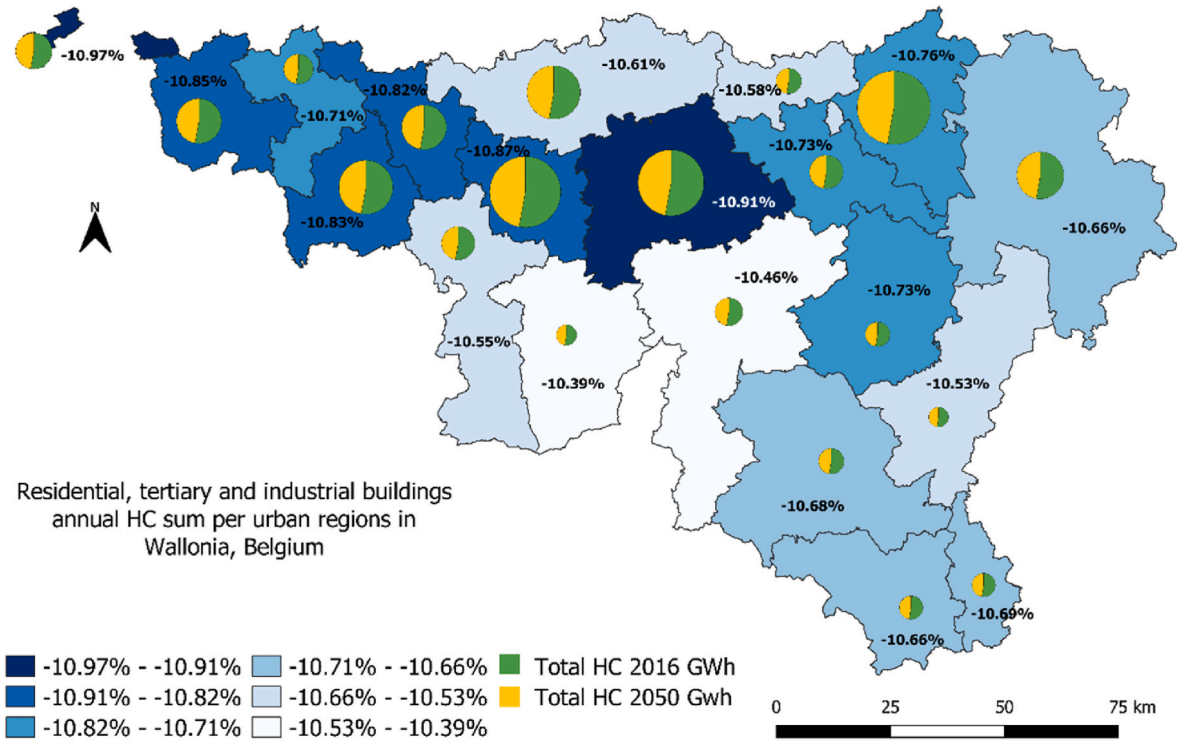

Fig. 16. Sum of the residential, tertiary, and industrial HC on the scale of the urban region. The diagrams show the difference in the Walloon building stock HC between 2016 and 2050 in % (graduated colour). (For interpretation of the references to colour in this figure legend, the reader is referred to the Web version of this article.)

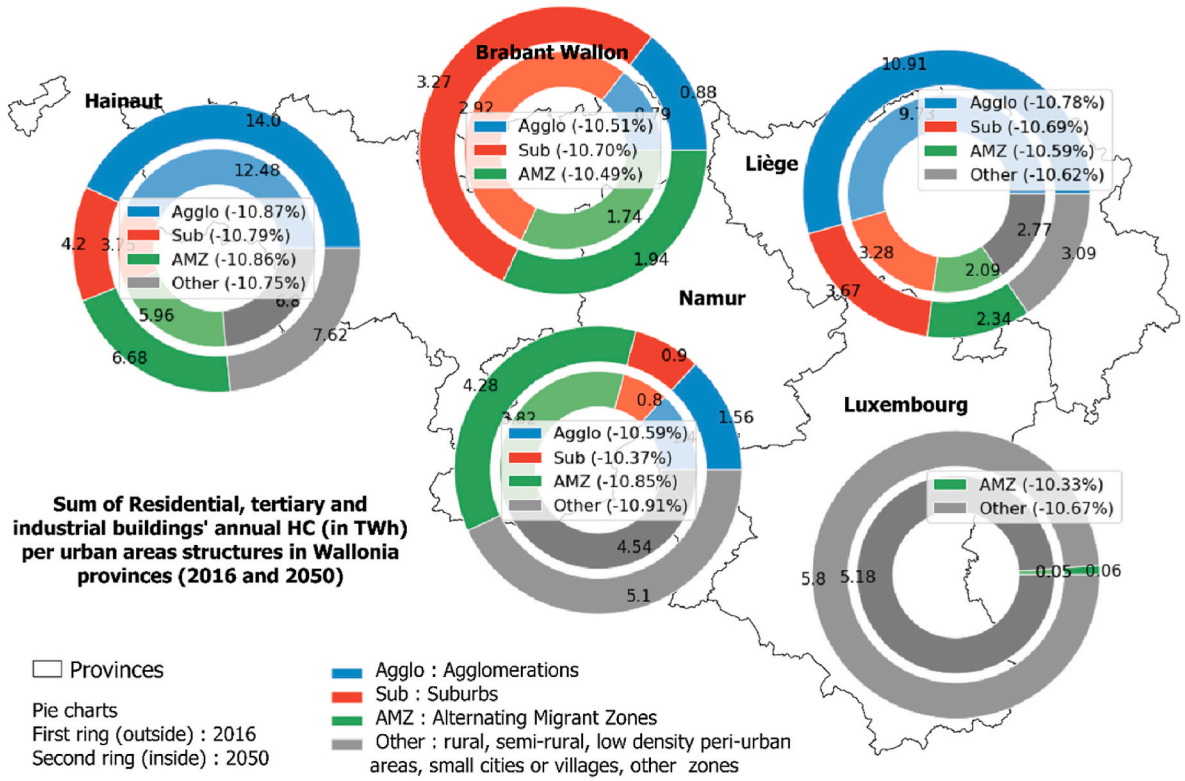

Fig. 17. Residential, tertiary, and industrial buildings HC for each province of Wallonia, split into urban areas as defined by Van Hecke et al. (Van Hecke et al., 2009).

investigated during this study, the visualization of the HC results shows variations at the urban region and municipality scales.

The applied methodologies in this study can also be used in any region of the World as long as the same kind of data exists. Nevertheless, buildings' energy consumption depends on many other factors. Apart from temperature changes and HDD, some researchers have found significant correlations of the HC with the energy prices and population income variables (Ruth and Lin, 2006), type and insulation of buildings (Kurekci, 2016), and national laws on heating (Moustris et al., 2011; Wang et al., 2009). As a solution to reduce the energy consumption of the building stock, the renovation of buildings, as found in the studies done by Ruellan et al. and Paiho et al. (Ruellan et al., 2021; Paiho et al., 2019), or the use of smart technologies on the municipality level are suggested. Assessing energy efficiency at the district scale presents several benefits compared to the building scale, such as reducing energy cost and implementing energy and sustainability strategies (Paiho et al., 2019). In further research, the deeper analysis of the HC forecast should be extended by including realistic and regulatory scenarios as well as multi-criteria analysis.

Data availability

- The temperature data can be found on: https://www.ncdc.noaa.gov/
- The HDD data are found on: https://energie.wallonie.be/fr/les-degres-jours-pour-vous-guider-a-travers-les-caprices-du-climat.html?IDC=9480&IDD=12611
- The Wallonia shapefiles can be accessed via: https://geoportail.wallonie.be/home.html

CRediT author statement

Antoinette Marie Reine Nishimwe: Literature review; Data collection and correction; Methodology; Software - programming and mapping; Analysis and discussion; Writing - Original draft preparation. **Sigrid Reiter**: Supervision; Correction; Writing - Revision of final draft.

Funding sources

This research, which is part of Wal-e-cities projects, is financed by the European Regional Development Fund (ERDF) and the Wallonia Region of Belgium.

Declaration of competing interest

The authors declare that they have no known competing financial interests or personal relationships that could have appeared to influence the work reported in this paper.

The authors declare the following financial interests/personal relationships which may be considered as potential competing interests:

Acknowledgements

The authors are very thankful to the European Regional Development Fund (ERDF) and the Walloon Region of Belgium, which financed the Wal-e-cities projects. The authors thank the LEMA research team of the University of Liège as well.

References

Aghelpour, P., Mohammadi, B., Biazar, S.M., 2019. Long-term monthly average temperature forecasting in some climate types of Iran, using the models SARIMA, SVR, and SVR-FA. Theor. Appl. Climatol. 138, 1471–1480. https://doi.org/10.1007/s00704-019-02905-w.

Almeida, L.M.M.C.E., Tam, V.W.Y., Le, K.N., 2021. Users' building optimal performance manual. Clean Responsible Consum 2, 100009. https://doi.org/10.1016/j.clrc.2021.100009.

Anđelković, A.S., Bajatović, D., 2020. Integration of weather forecast and artificial intelligence for a short-term city-scale natural gas consumption prediction. J. Clean. Prod. 266, 122096 https://doi.org/10.1016/J.JCLEPRO.2020.122096.

Anitha Kumari, K., Kumar Boiroju, N., Reddy, P.R., 2014. Forecasting of monthly mean of maximum surface air temperature in India. Int. J. Statistika Math. 9, 14–19.

Aras, H., Aras, N., 2004. Forecasting residential natural gas demand. Energy Sources 26, 463–472. https://doi.org/10.1080/00908310490429740.
Attia, S., Canonge, T., Popineau, M., Cuchet, M., 2022. Developing a benchmark model for renovated, nearly zero-energy, terraced dwellings. Appl. Energy 306, 118128. https://doi.org/10.1016/J.APENERGY.2021.118128.
Balyani, Y., Fazelniya, G., Bayat, A., 2012. A study and prediction of annuel temperature in shiraz using ARIMA model. Geogr Sp.
Bilous, I., Deshko, V., Sukhodub, I., 2018. Parametric analysis of external and internal factors influence on building energy performance using non-linear multivariate regression models. J. Build. Eng. 20, 327–336. https://doi.org/10.1016/j.jobe.2018.07.021.
Bourdeau, M., qiang, Zhai X., Nefzaoui, E., Guo, X., Chatellier, P., 2019. Modeling and forecasting building energy consumption: a review of data-driven techniques. Sustain. Cities Soc. 48 https://doi.org/10.1016/j.scs.2019.101533.
Box, G.E.P., Jenkins, G., 1976. Time Series Analysis: Forecasting and Control. This Week's Cit Class, p. 1.
Cholewa, T., Siuta-Olcha, A., Smolarz, A., Muryjas, P., Wolszczak, P., Guz, Ł., et al., 2021a. On the short term forecasting of heat power for heating of building. J. Clean. Prod. 307, 127232 https://doi.org/10.1016/J.JCLEPRO.2021.127232.
Cholewa, T., Siuta-Olcha, A., Smolarz, A., Muryjas, P., Wolszczak, P., Anasiewicz, R., et al., 2021b. A simple building energy model in form of an equivalent outdoor temperature. Energy Build. 236, 110766 https://doi.org/10.1016/j.enbuild.2021.110766.
Chung, J., Gulcehre, C., Cho, K., Bengio, Y., 2014. Empirical evaluation of gated recurrent neural networks on sequence modeling. NIPS 2014 Deep Learn. Represent. Learn. Work.
Day, A.R., Karayiannis, T.G., 1998. Degree-days: comparison of calculation methods. Build. Serv. Eng. Technol. 19, 7–13. https://doi.org/10.1177/014362449801900102.
Dombayci, Ö.A., 2010. The prediction of heating energy consumption in a model house by using artificial neural networks in Denizli-Turkey. Adv. Eng. Software 41, 141–147. https://doi.org/10.1016/j.advengsoft.2009.09.012.
Durmayaz, A., Kadıoğlu, M., Şen, Z., 2000. An application of the degree-hours method to estimate the residential heating energy requirement and fuel consumption in Istanbul. Energy 25, 1245–1256. https://doi.org/10.1016/S0360-5442(00)00040-2.
El-Mallah, E., Elsharkawy, S., 2016. Time-series modeling and short term prediction of annual temperature trend on coast Libya using the box-jenkins ARIMA model. Adv Res 6, 1–11. https://doi.org/10.9734/air/2016/24175.
Erdogdu, Erkan, 2010. Natural gas demand in Turkey. Appl. Energy 87, 211–219.
ETCCDI. ETCCDI/CRD climate change indices n.d. http://etccdi.pacificclimate.org/software.shtml. (Accessed 12 August 2020).
European Commission, 2016. Communication from the Commission to the European Parliament, the Council, the European Economic and Social Committee and the Committee of the Regions:An EU Strategy on Heating and Cooling. Brussels.
European Commission, 2017. Good practice in energy efficiency: for a sustainable, safer and more competitive Europe. Clean Energy All Eur 1–52. https://doi.org/10.2833/865683.
European Commission, 2018. The Energy Performance of Buildings Directive. Energy Perform Build Dir Factsheet, p. 1.
Fleiter, T., Steinbach, J., Ragwitz, M., Arens, M., Aydemir, A., Elsland, R., et al., 2016. Mapping and Analyses of the Current and Future (2020-2030) Heating/cooling Fuel Deployment (Fossil/renewables). https://doi.org/10.13140/RG.2.2.29193.75361.
Géron, Aurélien, 2019. Hands-On Machine Learning with Scikit-Learn, Keras and TensorFlow: Concepts, Tools, and Techniques to Build Intelligent Systems. O'Reilly Media, California.
Gorucu, F.B., Gumrah, F., 2004. Evaluation and forecasting of gas consumption by statistical analysis. Energy Sources 26, 267–276. https://doi.org/10.1080/00908310490256617.
Gorucu, F.B., Geriş, P.U., Gumrah, F., 2004. Artificial neural network modeling for forecasting gas consumption. Energy Sources 26, 299–307. https://doi.org/10.1080/00908310490256626.
Han, J.M., Ang, Y.Q., Malkawi, A., Samuelson, H.W., 2021. Using recurrent neural networks for localized weather prediction with combined use of public airport data and on-site measurements. Build. Environ. 192, 107601 https://doi.org/10.1016/j.buildenv.2021.107601.
Hong, T., Wang, Z., Luo, X., Zhang, W., 2020. State-of-the-art on research and applications of machine learning in the building life cycle. Energy Build. 212, 109831 https://doi.org/10.1016/j.enbuild.2020.109831.
Hossain, M.A., Chakrabortty, R.K., Elsawah, S., Ryan, M.J., 2021. Very short-term forecasting of wind power generation using hybrid deep learning model. J. Clean. Prod. 296, 126564 https://doi.org/10.1016/J.JCLEPRO.2021.126564.
Hyndman, R.J., Khandakar, Y., 2008. Automatic time series forecasting: the forecast package for R. J. Stat. Software 27, 1–22. https://doi.org/10.18637/jss.v027.i03.
Ibrahim, M.Z., Zailan, R., Ismail, M., Lola, M.S., 2009. Forecasting and time series analysis of air pollutants in several area of Malaysia. Am. J. Environ. Sci. 5, 625–632. https://doi.org/10.3844/ajessp.2009.625.632.
Johannesen, N.J., Kolhe, M., Goodwin, M., 2019. Relative evaluation of regression tools for urban area electrical energy demand forecasting. J. Clean. Prod. 218, 555–564. https://doi.org/10.1016/J.JCLEPRO.2019.01.108.
Kamruzzaman, M., Shahid, S., Islam, A.T., Hwang, S., Cho, J., Zaman, M.A.U., et al., 2021. Comparison of CMIP6 and CMIP5 model performance in simulating historical precipitation and temperature in Bangladesh: a preliminary study. Theor. Appl. Climatol. 145, 1385–1406. https://doi.org/10.1007/s00704-021-03691-0.
Karim, R., 2014. Seasonal ARIMA for forecasting sea surface temperature of the North zone of the Bay of Bengal. RRJoS 2, 23–31.
Khedhiri, S., 2016. Forecasting temperature records in PEI, Canada. Lett Spat Resour Sci 9, 43–55. https://doi.org/10.1007/s12076-014-0135-x.
Khotanzad, A., Elragal, H., 1999. Natural gas load forecasting with combination of adaptive neural networks. In: Proc. Int. Jt. Conf. Neural Networks, vol. 6. IEEE, pp. 4069–4072. https://doi.org/10.1109/ijcnn.1999.830812.
Khotanzad, A., Elragal, H., Lu, T.L., 2000. Combination of artificial neural-network forecasters for prediction of natural gas consumption. IEEE Trans. Neural Network. 11, 464–473. https://doi.org/10.1109/72.839015.
Kim, S., Kang, S., Ryu, K.R., Song, G., 2019. Real-time occupancy prediction in a large exhibition hall using deep learning approach. Energy Build. 199, 216–222. https://doi.org/10.1016/j.enbuild.2019.06.043.
Koch, M., Sun, H., 1999. Tidal and non-tidal characteristics of water levels and flow in the Apalachicola Bay, Florida. In: Coast. Eng. Mar. Dev. 4th Int. Conf. Comput. Model. Seas Coast. Reg. Lemn. May 1999, pp. 357–366.
Kumar, U., Jain, V.K., 2010. ARIMA forecasting of ambient air pollutants (O 3, NO, NO 2 and CO). Stoch. Environ. Res. Risk Assess. 24, 751–760. https://doi.org/10.1007/s00477-009-0361-8.
Kurekci, N.A., 2016. Determination of optimum insulation thickness for building walls by using heating and cooling degree-day values of all Turkey's provincial centers. Energy Build. 118, 197–213. https://doi.org/10.1016/j.enbuild.2016.03.004.
Liang, J., Qiu, Y (Lucy), Xing, B., 2022. Impacts of electric-driven heat pumps on residential electricity consumption: an empirical analysis from Arizona, USA. Clean Responsible Consum 4, 100045. https://doi.org/10.1016/j.clrc.2021.100045.
Liu, L.M., Lin, M.W., 1991. Forecasting residential consumption of natural gas using monthly and quarterly time series. Int. J. Forecast. 7, 3–16. https://doi.org/10.1016/0169-2070(91)90028-T.
Maggio, G., Cacciola, G., 2009. A variant of the Hubbert curve for world oil production forecasts. Energy Pol. 37, 4761–4770. https://doi.org/10.1016/j.enpol.2009.06.053.
Makridakis, S., Spiliotis, E., Assimakopoulos, V., 2018. Statistical and Machine Learning forecasting methods: concerns and ways forward. PLoS One 13. https://doi.org/10.1371/journal.pone.0194889.
Matzarakis, A., Thomsen, F., Mayer, H., 2009. Climate change and heating degree days in Freiburg im Breisgau, south-west Germany. Gefahrst. Reinhalt. Luft 69.
Moeeni, H., Bonakdari, H., 2017. Forecasting monthly inflow with extreme seasonal variation using the hybrid SARIMA-ANN model. Stoch. Environ. Res. Risk Assess. 31, 1997–2010. https://doi.org/10.1007/s00477-016-1273-z.
Monsell, B.C., 2007. The X-13a-S Seasonal Adjustment Program. US Census Bur Stat Res Div.
Moustris, K., Zacharia, P., Larissi, I., Nastos, P., Paliatsos, A., 2011. Cooling and heating degree-days calculation for representative locations within the greater Athens area, Greece. Proc 12th Conf Environ Sci Technol.
Murat, M., Malinowska, I., Gos, M., Krzyszczak, J., 2018. Forecasting daily meteorological time series using ARIMA and regression models. Int. Agrophys. 32, 253–264. https://doi.org/10.1515/intag-2017-0007.
Nam, K.J., Hwangbo, S., Yoo, C.K., 2020. A deep learning-based forecasting model for renewable energy scenarios to guide sustainable energy policy: a case study of Korea. Renew. Sustain. Energy Rev. 122, 109725 https://doi.org/10.1016/j.rser.2020.109725.
Nematchoua, M.K., Ricciardi, P., Orosa, J.A., Buratti, C., 2018. A detailed study of climate change and some vulnerabilities in Indian Ocean: a case of Madagascar island. Sustain. Cities Soc. 41, 886–898. https://doi.org/10.1016/j.scs.2018.05.040.
Neto, A.H., Fiorelli, F.A.S., 2008. Comparison between detailed model simulation and artificial neural network for forecasting building energy consumption. Energy Build. 40, 2169–2176. https://doi.org/10.1016/j.enbuild.2008.06.013.
Nishimwe, A.M.R., Reiter, S., 2021a. Estimation, analysis and mapping of electricity consumption of a regional building stock in a temperate climate in Europe. Energy Build. 253, 111535 https://doi.org/10.1016/j.enbuild.2021.111535.
Nishimwe, A.M.R., Reiter, S., 2021b. Building heat consumption and heat demand assessment, characterization, and mapping on a regional scale: a case study of the Walloon building stock in Belgium. Renew. Sustain. Energy Rev. 135, 110170 https://doi.org/10.1016/j.rser.2020.110170.
NOAA. National Climatic Data Center (NCDC): Archives of Oceanic, Atmospheric, Geophysical and Coastal Data. NOAA n.d. https://www.ncdc.noaa.gov/ (accessed August 12, 2020).
Nury, A., Koch, M., Alam, M., 2013. Time Series Analysis and Forecasting of Temperatures in the Sylhet Division of Bangladesh. UNSW, Sydney.
Paiho, S., Saastamoinen, H., Hakkarainen, E., Similä, L., Pasonen, R., Ikäheimo, J., et al., 2018. Increasing flexibility of Finnish energy systems—a review of potential technologies and means. Sustain. Cities Soc. 43, 509–523. https://doi.org/10.1016/j.scs.2018.09.015.
Paiho, S., Ketomäki, J., Kannari, L., Häkkinen, T., Shemeikka, J., 2019. A new procedure for assessing the energy-efficient refurbishment of buildings on district scale. Sustain. Cities Soc. 46 https://doi.org/10.1016/j.scs.2019.101454.
Ravnik, J., Jovanovac, J., Trupej, A., Vištica, N., Hriberšek, M., 2021. A sigmoid regression and artificial neural network models for day-ahead natural gas usage forecasting. Clean Responsible Consum 3, 100040. https://doi.org/10.1016/j.clrc.2021.100040.
RMI. Irm - normales climatiques à Uccle. n.d. https://www.meteo.be/fr/climat/climatologie-generale/normales-climatiques-a-uccle/temperature/indices-thermometriques/degres-jours. (Accessed 29 March 2021).
Ruellan, G., Cools, M., Attia, S., 2021. Analysis of the determining factors for the renovation of the Walloon residential building stock. Sustainability. https://doi.org/10.3390/su13042221.

Ruth, M., Lin, A.C., 2006. Regional energy demand and adaptations to climate change: methodology and application to the state of Maryland, USA. Energy Pol. 34, 2820–2833. https://doi.org/10.1016/j.enpol.2005.04.016.

Saloux, E., Candanedo, J.A., 2018. Forecasting district heating demand using machine learning algorithms. Energy Proc. 149, 59–68. https://doi.org/10.1016/j.egypro.2018.08.169. Elsevier Ltd.

Sarak, H., Satman, A., 2003. The degree-day method to estimate the residential heating natural gas consumption in Turkey: a case study. Energy 28, 929–939. https://doi.org/10.1016/S0360-5442(03)00035-5.

Spinoni, J., Vogt, J., Barbosa, P., 2015. European degree-day climatologies and trends for the period 1951-2011. Int. J. Climatol. 35, 25–36. https://doi.org/10.1002/joc.3959.

Spinoni, J., Vogt, J.V., Barbosa, P., Dosio, A., McCormick, N., Bigano, A., et al., 2018. Changes of heating and cooling degree-days in Europe from 1981 to 2100. Int. J. Climatol. 38, e191–208. https://doi.org/10.1002/joc.5362.

Suykens, J., Lemmerling, P.H., Favoreel, W., De Moor, B., Crepel, M., Briol, P., 1996. Modelling the Belgian gas consumption using neural networks. Neural Process. Lett. 4, 157–166. https://doi.org/10.1007/BF00426024.

Tektas, M., 2010. Weather forecasting using ANFIS and ARIMA models. Environ. Res. Eng. Manag. 51, 5–10.

Thaler, M., Grabec, I., Poredoš, A., 2005. Prediction of energy consumption and risk of excess demand in a distribution system. Phys. A Stat. Mech. its Appl. 355, 46–53. https://doi.org/10.1016/j.physa.2005.02.066.

Timmer, R.P., Lamb, P.J., 2007. Relations between temperature and residential natural gas consumption in the Central and Eastern United States. J. Appl. Meteorol. Climatol. 46, 1993–2013. https://doi.org/10.1175/2007JAMC1552.1.

Tonković, Z., Zekić-Sušac, M., Somolanji, M., 2009. Predicting natural gas consumption by neural networks. Teh Vjesn 16, 51–61.

UNFCCC, 2015. Report on the Structured Expert Dialogue on the 2013-2015 Review - United Nations, Framework Convention on Climate Change.

Valipour, M., 2015. Long-term runoff study using SARIMA and ARIMA models in the United States. Meteorol. Appl. 22, 592–598. https://doi.org/10.1002/met.1491.

Van Hecke, E., Halleux, J.-M., Decroly, J.-M., Mérenne-Schoumaker, B., 2009. Noyaux d'habitat et Régions urbaines dans une Belgique urbanisée.

Wang, X.K., Lu, W.Z., 2006. Seasonal variation of air pollution index: Hong Kong case study. Chemosphere 63, 1261–1272. https://doi.org/10.1016/j.chemosphere.2005.10.031.

Wang, X., Chen, D., Ren, Z., 2009. Assessment of climate change impact on residential building heating and cooling energy demand in Australia. Build. Environ.

Wang, J., Cui, Q., Sun, X., 2021. A novel framework for carbon price prediction using comprehensive feature screening, bidirectional gate recurrent unit and Gaussian process regression. J. Clean. Prod. 314, 128024 https://doi.org/10.1016/J.JCLEPRO.2021.128024.

Yamak, P.T., Yujian, L., Gadosey, P.K., 2019. A comparison between ARIMA, LSTM, and GRU for time series forecasting. In: ACM Int. Conf. Proceeding Ser. Association for Computing Machinery, New York, NY, USA, pp. 49–55. https://doi.org/10.1145/3377713.3377722.

Zhang, X., Yang, F., 2004. RClimDex (1.0) User Manual. Ontario.